

MUSCLE SPINDLE MORPHOLOGY IN THE TENUISSIMUS MUSCLE
OF THE GOLDEN SYRIAN HAMSTER

By

ROBERT MICHAEL PATTEN

B.Sc. (Kin), Simon Fraser University, 1986

A THESIS SUBMITTED IN PARTIAL FULFILLMENT OF
THE REQUIREMENTS FOR THE DEGREE OF
MASTER OF SCIENCE

in

THE FACULTY OF GRADUATE STUDIES

(Department of Anatomy)

We accept this thesis as conforming
to the required standard

THE UNIVERSITY OF BRITISH COLUMBIA

October 1990

© ROBERT MICHAEL PATTEN, 1990

In presenting this thesis in partial fulfilment of the requirements for an advanced degree at the University of British Columbia, I agree that the Library shall make it freely available for reference and study. I further agree that permission for extensive copying of this thesis for scholarly purposes may be granted by the head of my department or, by his or her representatives. It is understood that copying or publication of this thesis for financial gain shall not be allowed without my written permission.

Department of Anatomy

The University of British Columbia
Vancouver, Canada

Date 08 October, 1990

THESIS ABSTRACT

The tenuissimus is a long, thin hindlimb skeletal muscle which in hamsters contains about 200 extrafusal muscle fibers. Embedded in this richly innervated muscle is a continuous array of 16-20 closely packed muscle spindles suggesting that it may play a role in hindlimb proprioception. This high spindle density also makes the muscle ideal for the isolation and harvesting of these sensory receptors. In this correlative light and electron microscopic study, freshly frozen specimens were first prepared for serial microscopic analysis. Camera lucida reconstruction of spindle distribution showed a close proximity to the main artery and nerve in the central core of the muscle. Oxidative enzyme and myosin ATPase staining profiles were examined in both the intrafusal and extrafusal fiber populations. Type I and type II extrafusal fibers were present in even numbers and were distributed evenly throughout muscle cross-sections. Enzyme staining varied along the lengths of the three intrafusal fiber types. The fine structure of spindles was examined using transmission (TEM), conventional scanning (SEM), and high resolution scanning electron microscopy (HRSEM). For conventional SEM, isolated spindles were first fixed in 2.5% buffered glutaraldehyde, followed by 1% osmication, and mechanical disruption of the outer capsule under the dissecting microscope. Preparation for HRSEM included aldehyde/osmium fixation and freeze-cleavage of entire tenuissimus muscles in liquid N₂. Selective extraction of the cytosol with 0.1% OsO₄ permitted the visualization of numerous intracellular structures. In these specimens, the capsular sleeve showed a multilayered pattern of vesicle-laden cells with variant surface topography in certain locations. Punctate sensory nerve endings adhered intimately to the surfaces of underlying intrafusal fibers in the equatorial and juxtaequatorial regions. By TEM and HRSEM these endings appeared crescent-shaped and were enveloped by external laminae. Each profile contained a plethora of mitochondria and cytoskeletal organelles. The methodology used in this study provides, for the first time, a three-dimensional view of the exquisite cytological architecture of this neuromuscular receptor.

TABLE OF CONTENTS

THESIS ABSTRACT	ii
LIST OF FIGURES	iv
LIST OF ABBREVIATIONS	v
ACKNOWLEDGMENTS	vii
GENERAL INTRODUCTION AND OUTLINE OF THESIS OBJECTIVES	
Historical Background	1
Morphology of Mammalian Muscle Spindles	2
The Tenuissimus Muscle	7
High Resolution Scanning Electron Microscopy	9
Thesis Objectives	11
CHAPTER 1: LIGHT MICROSCOPIC ASSESSMENT OF THE HAMSTER TENUISSIMUS	
Abstract	12
Introduction	13
Methods	15
Observations	19
Discussion	24
CHAPTER 2: ELECTRON MICROSCOPY OF MUSCLE SPINDLES IN THE HAMSTER TENUISSIMUS	
Abstract	29
Introduction	30
Methods	32
Observations	35
Discussion	41
CONCLUSIONS AND FUTURE DIRECTIONS	50
LITERATURE CITED	52

LIST OF FIGURES AND TABLE

FIGURE 1	Light Micrograph of the Tenuissimus Muscle	6 2
FIGURE 2	Light Micrograph of a Muscle Spindle in the Juxtaequatorial Zone	6 2
FIGURE 3	Light Micrograph of a Tandem Muscle Spindle	6 2
FIGURE 4	Longitudinal Reconstruction of Muscle Spindle Distribution	6 3
TABLE I	Summary of Muscle Spindle Quantitative Data	6 3
FIGURE 5-7	Myosin ATPase and NADH-TR Staining of Intrafusal Fibers	6 5
FIGURE 8	Schematic Diagram of Intrafusal Fiber Myosin ATPase Staining Patterns	6 7
FIGURE 9	Schematic Diagram of Intrafusal Fiber NADH-TR Staining Patterns	6 7
FIGURE 10	Light Micrograph of an Isolated Muscle Spindle	6 9
FIGURE 11	Isolated Muscle Spindle Stained With NBD-Phalloidin	6 9
FIGURE 12	High Resolution SEM of a Muscle Spindle in the Equatorial Region	7 1
FIGURE 13	High Resolution SEM Stereo Pair of a Muscle Spindle in the Juxtaequatorial Region	7 3
FIGURE 14	Conventional SEM of the Spindle Capsule and Intrafusal Fibers	7 5
FIGURE 15	Conventional SEM of the Outer Spindle Capsule and Perineurial Sheath	7 5
FIGURE 16-18	High Resolution SEM Views of the Muscle Spindle Outer Capsule	7 7
FIGURE 19-20	High Resolution SEM Views of the Muscle Spindle Inner Capsule	7 9
FIGURE 21	High Resolution SEM of a Fusimotor Nerve Ending	8 1
FIGURE 22	High Resolution SEM of a Sensory Nerve Ending	8 1
FIGURE 23-24	SEM and TEM Views of a Sensory Nerve Terminal on an Intrafusal Fiber	8 3
FIGURE 25-26	High Resolution SEM Stereo Pairs of Spindle Sensory Nerve Endings	8 5
FIGURE 27	High Magnification SEM of a Spindle Sensory Nerve Ending	8 7

LIST OF ABBREVIATIONS

ATPase	Adenosine Triphosphatase
Ca ²⁺	Calcium
cm	Centimeter(s)
CO ₂	Carbon Dioxide
° C	Degrees Centigrade
DMSO	Dimethylsulphoxide
g	Gram(s)
HCL	Hydrochloric acid
H & E	Hematoxylin and Eosin
h r	Hour(s)
HRSEM	High Resolution Scanning Electron Microscopy/Microscopic
KCl	Potassium chloride
KH ₂ PO ₄	Monobasic Potassium Phosphate
kV	Kilovolt(s)
M	Molar/Molarity
mA	Milliamp(s)
mg	Milligram(s)
μm	Micrometer(s)
μm ²	Micrometers squared
min	Minute(s)
mm	Millimeter(s)
mM	Millimolar
N	Normal/Normality
N ₂	Nitrogen
Na ⁺	Sodium

Na ₂ HPO ₄	Dibasic Sodium Phosphate
NaCl	Sodium Chloride
NADH-TR	Nicotinamide Adenine Dinucleotide Tetrazolium Reductase
NaOH	Sodium Hydroxide
NBD	7-Nitrobenz-2-Oxa-1,3-Diazole
nm	Nanometer(s)
OsO ₄	Osmium Tetroxide
p ₁	Plate 1
p ₂	Plate 2
PMC	Parallel Muscle Combination
PBS	Phosphate-Buffered Saline
sec	Second(s)
SEM	Scanning Electron Microscope/Scanning Electron Microscopic
SR	Sarcoplasmic Reticulum
TEM	Transmission Electron Microscope/Transmission Electron Microscopic
T-tubule	Transverse-Tubule
wt	Weight

ACKNOWLEDGMENTS

There are a number of people to whom I owe my gratitude. First and foremost I wish to extend my sincere thanks to my advisor Dr. William Ovalle. I consider it a privilege to have had the opportunity to work with him. His endless patience, liberal guidance and sincere interest in my overall education are greatly appreciated. Thanks also to the other members of my committee, Dr. Bernard Bressler and Dr. Bruce Crawford and to Dr. Wayne Vogl and Dr. Pierre Dow for their interest, support and encouragement.

I gratefully acknowledge Drs. Peter J. Lea and Martin J. Hollenberg for their technical advice and for use of their HRSEM facilities in the Department of Anatomy at the University of Toronto. I also wish to thank Mary Major of the Department of Metals and Materials Engineering for her assistance.

My thanks also to the Department of Anatomy for creating an environment that encourages scientific curiosity and promotes intellectual growth. A special thanks goes to Dr. Don Hedges for all his encouragement and advice when it really counted.

Finally, thanks to my wife Tracy and to my family for all their patience, understanding and encouragement. Without their support, none of this would have been possible.

This work was supported by grants to Dr. W.K. Ovalle from NSERC and the Muscular Dystrophy Association of Canada and by a University Graduate Fellowship to R.M. Patten.

GENERAL INTRODUCTION AND OUTLINE OF THESIS OBJECTIVES

Historical Background

Muscle spindles are specialized sensory stretch receptors situated in the perimysial connective tissue of skeletal muscle. Each receptor lies in-parallel with the surrounding extrafusal fiber population and serves to monitor active and passive changes in muscle length. There are three main components that make up a muscle spindle, a group of specialized muscle fibers known as intrafusal fibers, an intricate motor and sensory nervous innervation, and a complex epithelial and connective-tissue capsule. For orientation and descriptive purposes, the spindle can be described in terms of three regions or zones. The equatorial zone represents the central or widest portion of the receptor. In this region, both an inner and an outer spindle capsule are present, separated from each other by a prominent periaxial space. The polar regions represent the two tapered ends of the receptor. Here intrafusal fibers are solely invested by an outer capsule. Regions midway between equatorial and polar zones are referred to as juxtaequatorial.

The study of muscle spindles dates back to the middle of the 19th century, when Weismann (1861) first recognized these encapsulated structures as discrete entities. Kühne (1864) noted their peculiar fusiform shape and gave them the name *Muskelspindel*, a name that persists to this day. Convincing proof of the spindle's sensory function came near the end of the 19th century, largely through the work of Sherrington (1894) and Ruffini (1898). A thorough demonstration of its fusimotor innervation was not achieved until well into the 20th century. It was Leksell (1945) who finally provided definitive proof that the small (gamma) motor axons of a muscle nerve, observed earlier by Eccles and Sherrington (1930), actually innervated muscle spindles.

The first detailed and descriptive assessment of muscle spindle ultrastructure as seen with the transmission electron microscope was carried out by Merrillees (1960). Studying muscle spindles in lumbrical muscles of the rat, Merrillees (1960) ushered in a new era of muscle spindle research that would attempt to equate the fine structure of these unique receptors with their functions. The work of Merrillees (1960) was followed soon afterwards by a series of ultrastructural studies that examined various aspects of spindle morphology in different species (Katz, 1961; Karlsson et al., 1966; Landon, 1966; Adal, 1969; Corjava et al., 1969; Banker and Girvin, 1971; Ovalle, 1971, 1972a, b; Smith and Ovalle, 1972; James and Meek, 1973; Barker, 1974). These studies have collectively formed the framework for our current understanding of how muscle spindles are put together.

The Morphology of Mammalian Muscle Spindles

The Capsule

The muscle spindle capsule has both an inner and an outer component that differ from each other both in structure and in location (Merrillees, 1960; Landon, 1966; Corjava et al., 1969). The outer spindle capsule is a lamellated structure that gives the receptor its characteristic fusiform shape. The capsular lamellae are composed of layers of thin and flattened epithelial-like cells that are arranged in concentric fashion around the receptor. An abundant number of longitudinally and circumferentially oriented collagen fibrils are found interspersed between the cell layers and on the outer surface of the capsule (Merrillees, 1960; Landon, 1966). The ultrastructure of these outer capsule cells was first described by Merrillees (1960) who referred to them as *capsular sheet cells*. Within their cytoplasm are numerous cellular organelles including mitochondria, rough-surfaced endoplasmic reticulum, and large numbers of pinocytotic vesicles. Each capsular cell is surrounded by an external lamina and closely interdigitates with its neighbors to form a continuous layer around the receptor. Attenuated processes of the same concentric layer abut and are often linked by

intercellular junctions (Merrillees, 1960; Landon, 1966; Corjava et al., 1969; Kennedy and Yoon, 1979; Dow et al., 1980).

The outer spindle capsule is thought to be continuous with, and structurally similar to, the perineurial sheath of peripheral nerve (Merrillees, 1960; Shantha and Bourne, 1968; Shantha et al., 1968; Corjava et al., 1969). Kennedy and Yoon (1979) and Dow and co-workers (1980) have shown that the capsule, like the peripheral nerve perineurium, acts as a barrier to the diffusion of macromolecular tracers.

The inner spindle capsule or *axial sheath* (Barker, 1974) consists of flattened and contiguous cells that morphologically (Barker, 1974; Low, 1976) and functionally (Edwards, 1975; Dow et al., 1980) resemble the endoneurial cells of peripheral nerve. Inner capsule cells are most prominent in the equatorial region where they form an elaborate sheath around the intrafusal fibers and their sensory nerve endings. In some instances, thin cytoplasmic processes emanate from the cell bodies of these cells to further envelop and enclose the intrafusal fibers into individual compartments (Ovalle and Dow, 1983). Three types of intercellular specializations are known to occur between inner capsule cells. These include intermediate junctions (zonulae adherentes), tight junctions (zonulae occludentes), and gap junctions (Ovalle and Dow, 1983). Unlike outer capsule cells, cells of the inner capsule lack an external lamina although collagen and elastic fibrils are known to occupy the paracellular regions (Cooper and Gladden, 1974).

In the equatorial region, a prominent periaxial space separates the inner capsule and the intrafusal fibers from the surrounding outer spindle capsule. This space is thought to contain a thin mucopolysaccharide gel rich in hyaluronic acid (Brzezinski, 1961a, b; James, 1971; Fukami, 1982, 1986). The precise origin and function of this periaxial gel has not yet been pinpointed although it may contribute to the insulation and mechanical protection of the underlying sensory nerve endings (Barker and Banks, 1986).

Intrafusal Fibers

Muscle spindles contain two distinctly different intrafusal fiber types that can be identified on the basis of their appearance and according to the arrangement of nuclei in their central equatorial regions. Nuclear bag fibers contain large collections of tightly packed, vesicular nuclei in the equatorial region. Nuclear chain fibers, in contrast, contain a single row of nuclei that are centrally located within the fibers, surrounded by a peripheral layer of myofibrils. Bag fibers can be further classified as bag₁ and bag₂ based on certain histochemical features. Bag₁ fibers tend to have a low glycogen content (Banks et al., 1977) and the myosin ATPase activity of these fibers is acid-stable but alkaline-labile (Ovalle and Smith, 1972). The glycogen content of bag₂ fibers is medium and the myosin ATPase is both acid and alkaline-stable. In most spindles bag fibers are the longest, and bag₂ fibers are generally longer than bag₁ fibers (Kucera, 1982a). Some spindles contain chain fibers that are extraordinarily long. They are known to extend beyond the limits of the capsule and they insert into the perimysial connective tissue along with the bag fibers. These intrafusal fibers are called *long chain* fibers and were first described by Harker and co-workers (1977). Myosatellite cells are often seen in association with bag₂ fibers but are rarely seen in association with chain fibers (Banks, 1981a).

At the ultrastructural level, further differences in intrafusal fiber morphology have been noted. Nuclear chain fibers are reported to have abundant sarcoplasm rich in glycogen and large mitochondria (Merrillees, 1960). The sarcoplasmic reticulum is highly developed and triads, diads, and pentads of the sarcotubular system are frequently encountered (Ovalle, 1971). In the equatorial and juxtaequatorial regions two or three chain fibers can sometimes share the same external lamina and they are often linked by intercellular junctions (Corjava et al., 1969).

In contrast to chain fibers, nuclear bag fibers have a less well developed sarcotubular system and there is little intermyofibrillar sarcoplasm or glycogen. Mitochondria are also fewer and smaller than those in chain fibers. Bag₁ fibers usually have a thicker Z band but lack a distinct M line. Bag₂ fibers have an M line that is evident in all regions except for the equatorial zone (Banks et al., 1977). In the polar regions, paracellular elastic fibrils are commonly found associated with bag₂ fibers (Cooper and Gladden, 1974).

Nervous Innervation

Muscle spindles have a complex nervous innervation that is both motor and sensory in nature. The sensory component is made up of both primary and secondary nerve endings (Ruffini, 1898). Primary endings are connected to large-diameter 1a afferent nerve axons. Each muscle spindle is supplied by a single 1a afferent fiber that pierces the outer capsule and divides to terminate on all three intrafusal fiber types. The terminations usually lie along the densely nucleated regions of the intrafusal fibers (Ruffini, 1898) in the form of spirals, half rings and, in some cases, complete rings (Banks et al., 1982; Banks, 1986). Accordingly, these terminations are sometimes termed *primary* or *annulospiral endings*. In the cat, the terminations cover 33-37% of the bag₁ fiber surface, 24-25% of the bag₂ fiber surface and 5-12% of the surface of individual chain fibers (Banks et al., 1982; Banks, 1986). In some cases, sensory terminals cross from one intrafusal fiber to another. Such an arrangement usually occurs between adjacent chain fibers and is referred to as a *sensory cross-terminal* (Adal, 1969).

Many, but not all, spindles are innervated in addition by one or more group II afferent nerve fibers. These sensory fibers usually terminate on one or both sides of the primary endings and are referred to as *secondary endings*. These sensory endings usually consist of less regular spiral terminations around chain fibers and spray-like terminations on bag fibers (Boyd and Smith, 1984). The majority of secondary endings are associated with chain fibers;

bag₂ fibers receive up to 20% of the total number of secondary terminals while no more than 10% lie on bag₁ fibers (Banks et al., 1982). In the cat *tenuissimus*, the total terminal contact area of secondary endings has been estimated to be 16-22% on individual chain fibers, 17% on bag₂ fibers and 8% on bag₁ fibers (Banks et al., 1982).

Ultrastructurally, there are very few differences between primary and secondary endings. Both are packed with mitochondria, neurofilaments, microtubules, and axoplasmic vesicles. Moreover, both primary and secondary endings lie in close apposition to the underlying intrafusal fibers. Some terminals, particularly those of the primary variety, are deeply indented onto the intrafusal fiber surface (Landon, 1966). The intrafusal fiber's external lamina does not extend through the intercellular gap, but instead covers the outer portion of each ending in blanket-like fashion. Moreover, there is no Schwann cell present in these regions (Merrillees, 1960), a feature that distinguishes sensory endings from motor terminals.

The highly complex afferent nervous innervation has been the subject of considerable controversy for many years. Noteable reviews in this regard have been published (Boyd, 1981; Boyd and Smith, 1984; Barker and Banks, 1986). It is generally accepted that there are two forms of motor innervation to intrafusal fibers. The gamma innervation consists of small-diameter efferent nerve axons that innervate the intrafusal fibers exclusively. They have been estimated to account for 30% of the nerve fibers in the ventral roots (Boyd and Smith, 1984) and are sometimes referred to as *fusimotor* axons (Barker, 1974). There is also a sparse innervation of spindles by beta or *skeleto-fusimotor* axons (Barker, 1974). These efferent fibers have collateral branches that also innervate neighboring extrafusal fibers in the same muscle. Both gamma and beta efferents can be subdivided into static and dynamic subgroups based upon the intrafusal fibers they innervate and how they influence the response of the receptor to stretch.

Efferent nerve endings are usually restricted to the polar and extracapsular regions of intrafusal fibers although some also reside in the juxtaequatorial regions. Each bag-fiber pole can receive two to three motor endings, whereas each chain-fiber pole usually receives only one (Barker and Banks, 1986). Generally speaking, gamma-static axons can innervate bag₂ fibers, chain fibers, or both. Gamma-dynamic axons usually only innervate bag₁ fibers as do beta-dynamic axons. Beta-static fibers are often restricted to the extracapsular regions of long chain fibers (Kucera, 1980a). Variations of this general plan frequently occur amongst different species.

Finally, three different types of motor nerve ending can be distinguished based upon the degree of their indentation onto intrafusal fiber surfaces, the form and location of their axon terminals, and the diameter and mode of branching of the terminal axon. These endings have been termed *trail*, *plate₁* and *plate₂* (Barker et al., 1970). It is thought that beta axons terminate in p₁ plates, gamma-static axons in trail endings and gamma-dynamic axons in p₂ plates (Barker et al., 1980; Banks et al., 1985).

The Tenuissimus

The tenuissimus muscle of the cat is presently one of the most common muscles used for muscle spindle research. Aptly named for its long attenuated appearance, the tenuissimus is also found in the rabbit (Bensley, 1921; Walker, 1980), dog (Miller, 1964), mink (Walker, 1980), and hamster (Desaki and Uehara, 1983). Also known as the *tensor fasciae cruris* (Bensley, 1921) or *abductor cruris caudalis* (Miller, 1964; Walker, 1980), the tenuissimus runs parallel to the sciatic nerve in the leg just below the caudofemoralis and the biceps femoris muscles. It originates on a caudal or sacral vertebrae and has a common insertion with the biceps femoris on the tibia and adjacent crural fascia (Walker, 1980). The tenuissimus is thought to function in a synergistic fashion with the biceps femoris in producing extension and

abduction of the thigh and flexion of the knee (Miller, 1964; Walker, 1980; Lev-Tov et al., 1988).

The tenuissimus has been studied more extensively in the cat than in other animals. Its macroscopic appearance and anatomical relations were first described by Adrian (1925), whereas Boyd (1956) was the first to describe it microscopically. In the cat, the muscle is usually 15-20 cm long, 3-4 mm wide and 1 mm thick (Lev-Tov et al., 1988). It contains between 700 and 1300 extrafusal muscle fibers (Boyd, 1956) that can be classified histochemically as Type I, Type IIA, and Type IIB (Lev-Tov et al., 1988). The myofibers, which are 20-30 mm in length on average (Loeb et al., 1987), are arranged in serial or overlapping arrays that are parallel with the longitudinal axis of the muscle. Myofibers that occupy the midbelly region of the muscle have ends that are finely tapered and lie closely apposed to the surfaces of neighboring extrafusal fibers (Loeb et al., 1987). Muscle fibers that are situated near the origin or the insertion of the muscle have only one end that is finely tapered, whereas the other end is attached to tendon in typical fashion (Loeb et al., 1987).

The microvasculature of the tenuissimus in the cat and in the rabbit has been studied in detail by Eriksson and Lisander (1972), Eriksson and Myrhage (1972) and Miyoshi and Kennedy (1979). According to Eriksson and Myrhage (1972), the blood vessels that supply the tenuissimus do not supply any other muscles and they do not anastomose with vessels from other muscles. There is usually one central artery and one central vein that lie closely apposed to each other and run parallel to the muscle fibers. Transverse arterioles and venules branch off at right angles from the central vessels and, after several generations of branching, give rise to capillaries that are again aligned in-parallel with the muscle fibers. The blood supply to muscle spindles in the tenuissimus is separate from that to the adjacent extrafusal fibers (Miyoshi and Kennedy, 1979). The arterial pathway leading to spindle capillaries is shorter and more direct, and the spindle capillaries anastomose with each other to form a vascular loop near the sensory nerve endings (Miyoshi and Kennedy, 1979).

Although Hunt and Kuffler (1951) used the tenuissimus to investigate the electrophysiological properties of muscle spindles, Boyd (1956) was the first to point out its usefulness for both the physiological and morphological assessment of these receptors. Boyd (1956) demonstrated that, in the cat, the tenuissimus contains 14-16 spindles that are 4-12 mm in length and are arranged in serial fashion along the length of the muscle, in close proximity to the main nerve supply.

High Resolution Scanning Electron Microscopy

Since it first became available in the mid 1960's, the scanning electron microscope has been restricted for the most part, to the morphological evaluation of cell and tissue surfaces (Hollenberg and Erickson, 1973). The limited resolution of early instruments, combined with the thick metallic coating needed on specimens, made the observation of fine structural detail somewhat difficult. In recent times this has changed considerably. A new technique known as high resolution scanning electron microscopy (HRSEM) has made it now possible to observe fine intracellular details at a resolution that rivals that of the conventional transmission electron microscope (Hollenberg and Lea, 1988).

The evolution of HRSEM is based upon two important developments. The first is the improvements made in the design and resolving power of modern scanning electron microscopes. The second is the remarkable new technique of tissue preparation pioneered by Tanaka (1972) and Tanaka and Mitsushima (1984) and recently modified and improved by Hollenberg and co-workers (1989). There are two basic principles involved in this technique. The first is the fracturing and opening up of cells and the second is the selective removal of the cell cytoplasm. Previously, even if cells were fractured open properly it was often difficult to obtain a clear SEM view because intracellular structures were usually hidden within the cytoplasmic matrix. To alleviate this problem, Tanaka and Mitsushima (1984)

developed a technique of cytoplasmic maceration which they named the *osmium-DMSO-osmium method*.

Briefly, this method involves (1) the quick freezing in liquid nitrogen of tissue fixed initially with weak aldehydes and osmium, (2) the cracking open of the tissue with a hammer and a razor blade, (3) the thawing and postfixation of the tissue, (4) the partial extraction of the tissue using dilute osmium tetroxide, and (5) critical point drying and coating with a thin layer of a highly conductive metal, such as gold. This extraction procedure leaves intracellular organelles, nuclear chromatin, and cellular membranes intact.

How it is that the osmium successfully removes the cytoplasmic matrix but leaves membranous structures well preserved is somewhat unclear. Tanaka and Mitsushima (1984) suggest that proteins in the cytoplasmic matrix are decomposed by the osmium to a state that allows them to diffuse out through the fractured surface of the cell. Membranous proteins are presumably protected by the lipid molecules that surround them. The nature of this enhanced solubility has recently been reviewed by Sjöstrand (1989). He suggests that the binding of osmium to protein molecules adds strong positive charges to the polypeptide chains causing them to unfold. It also enhances their ability to bind water and to interact with each other to form a gel. It is this gelation that makes the proteins in the cytosol more soluble (Porter and Kallman, 1953).

Is the ultrastructure of the remaining cellular elements altered by the cytosol extraction procedure? To address this question, Lea and Hollenberg (1988) recently compared liver tissue prepared for TEM with liver tissue prepared for HRSEM. They were unable to detect any appreciable differences either in the quality of fixation or in ultrastructural preservation between the two techniques.

In summary, the use of HRSEM can reveal ultrastructural details not obtainable by other current methodologies. It is a powerful technique that provides a new and different way

of examining and appreciating cellular ultrastructure. Furthermore, the use of stereo-pair micrographs can be used to demonstrate the three-dimensional organization of cells and tissues. In light of this, it would be useful to apply this technique to the study of muscle spindles.

Thesis Objectives

Although the literature is replete with studies documenting the fine structure of muscle spindles, very little attention has been paid to the study of these sensory receptors from a three-dimensional perspective. To more clearly understand the function of these complex receptors it is essential that further details regarding their structural make up are elucidated. A scanning electron microscopic evaluation of muscle spindles would provide valuable information in this regard. Such a study would involve the microdissection and isolation of individual spindles and therefore the first step would be to determine a suitable muscle model. The tenuissimus muscle of the hamster has been chosen to fulfill this role.

The project has been divided into studies. The first chapter of this thesis deals with the morphological, histochemical, and quantitative parameters associated with the hamster tenuissimus and its muscle spindles. The second chapter attempts to utilize the techniques of conventional and high resolution scanning electron microscopy for the evaluation of muscle spindle ultrastructure. It is the goal of the thesis to address a number of fundamental questions. How is the hamster tenuissimus organized morphologically? Is this muscle similar to its counterpart in the cat in terms of its muscle spindle content? Can the hamster tenuissimus be used for the microdissection and isolation of these receptors for further scanning electron microscopic evaluation? Finally, what is the fine structure of muscle spindles when examined three-dimensionally and how does this compare to what is known from previously published ultrastructural studies?

CHAPTER 1

LIGHT MICROSCOPIC ASSESSMENT OF THE HAMSTER TENUISSIMUS

ABSTRACT

Muscle spindles and extrafusal fibers in the tenuissimus muscle of mature golden syrian hamsters were studied morphologically and quantitatively using several light microscopic techniques. Muscle spindles were identified in serial-transverse frozen-sections of whole muscles stained with hematoxylin and eosin. Five tenuissimus muscles were examined from origin to insertion, and the locations of individual receptors were plotted in camera-lucida reconstructions. Spindles were found in close proximity to the main artery and nerve in the central core of each muscle. A range of 16-20 receptors and an average of 236 extrafusal fibers were noted. The mean muscle spindle index (the total number of spindles per gram of muscle weight) was 502.7 and the average spindle length was 7.5 mm. Oxidative enzyme and myosin ATPase staining profiles were also evaluated in the intrafusal and extrafusal fiber populations in each muscle. Even numbers of type I and type II extrafusal fibers were distributed homogeneously throughout all muscle cross-sections. Histochemical staining patterns varied along the lengths of the three intrafusal fiber types. Nuclear chain fibers possessed staining properties similar to the type II extrafusal fibers and exhibited no regional variations. Bag₁ fibers displayed staining variability, particularly when treated for myosin ATPase activity under acid preincubation conditions. Some spindles were isolated under darkfield illumination and then treated with NBD-phalloidin to detect filamentous actin by fluorescence microscopy. In these preparations, a registered actin banding-pattern was observed in the sarcomeres of the intrafusal fibers and variations in the intensity of banding were noted amongst different fibers. The high spindle density observed in this muscle suggests that the hamster tenuissimus may function in hindlimb proprioception.

INTRODUCTION

The tenuissimus muscle in the cat has been studied extensively by light microscopy (Boyd, 1956; Loeb et al., 1987; Lev-Tov et al., 1988). Considerably less is known about the morphology of its counterpart in the hamster. In an ultrastructural study of intrafusal fibers of muscle spindles, Desaki and Uehara (1983) made the first observations regarding the light microscopic appearance of the tenuissimus in the hamster. They noted its distinct oval-shaped cross-sectional profile, and they reported that it contained about 100 extrafusal fibers and many muscle spindles. Aside from this report, no studies have been undertaken to assess the histochemical and quantitative features of the hamster tenuissimus and its muscle spindle population.

In the cat, the tenuissimus is a long and delicate hindlimb muscle closely associated with the much larger biceps femoris (Boyd, 1956; Walker, 1980) that reportedly contains between 700 and 1300 extrafusal fibers (Boyd, 1956). Such an anatomical arrangement, coupled with its rich supply of serially organized muscle spindles (Boyd, 1956), has led investigators to postulate that the muscle contributes minimally to mechanical actions about the hip and knee (Lev-Tov et al., 1988). If this is so, the question arises as to what purpose the tenuissimus might actually serve. To address this question, a more detailed assessment of its histological organization and internal architecture is required.

Due to its extremely high spindle content, the cat tenuissimus has also been utilized extensively in studies documenting the light microscopic and histochemical profiles of these unique receptors (Barker et al., 1976, 1977; Kucera, 1980a, 1981, 1982a, b, 1983). Whether the hamster tenuissimus can be utilized in a similar fashion remains to be determined.

The present study was undertaken to assess the light microscopic characteristics of the hamster tenuissimus and its muscle spindles. It was also initiated as part of a prelude to a more extensive electron microscopic study of muscle spindle ultrastructure. The morphological and histochemical profiles of both the intrafusal and extrafusal fiber populations were assessed and the density and distribution of spindles were also determined. Moreover, the possible role that the muscle plays in the hamster hindlimb along with its suitability as a model for the study of isolated mammalian muscle spindles, was also considered. A preliminary report of a portion of this work has been published (Patten and Ovalle, 1990).

METHODS

Seven adult male Golden Syrian Hamsters (*Mesocricetus auratus*) were used. Animals were kindly provided by Dr. R. Shah, in the Department of Oral Biology at the University of British Columbia, from breeding pairs originally obtained from Simonson's Laboratories, Gilroy, CA. A total of 102 spindles from 7 muscles were examined.

Histochemistry

Animals were first killed with an overdose of chloroform, and then quickly weighed on a Precisa 200C-2000D1 electronic balance. The left tenuissimus from each animal was rapidly exposed by dissection, the superficial fascia was removed, and the entire muscle was then quickly excised. Dissected muscles were placed on surgical gauze moistened with 0.9% saline and wet muscle weights were determined using a Mettler AE163 digital analytical balance. Each muscle was then sandwiched between two thin slices of hamster liver, pinned through its tendons to a cork chuck and immersed for 30 sec in isopentane cooled to -160°C in liquid N_2 . Frozen specimens were transferred to a Forma Scientific Bio Freezer maintained at -60°C for storage until sectioning and subsequent staining. Prior to sectioning, muscle blocks were mounted on metal chucks with O.C.T. embedding medium (Miles Laboratories, Naperville, Ill.) and allowed to equilibrate to -20°C in a Histostat 975C cryostat microtome (AO Scientific Instruments, Buffalo, NY). Five muscles were cut with a metal knife in serial fashion from origin to insertion at a section thickness of $10\ \mu\text{m}$. At $100\ \mu\text{m}$ intervals, five consecutive transverse-sections were collected on separate glass coverslips and air dried for 1 hr. Adjacent sections were either stained with hematoxylin and eosin (H & E), treated to detect nicotinamide adenine dinucleotide tetrazolium reductase (NADH-TR) activity (Novikoff et al., 1961), or treated to detect myosin adenosine-triphosphatase (ATPase) activity at acid (pH 4.2 and pH 4.6) and alkaline (pH 9.4) preincubations (Dubowitz and Brooke, 1973). The original myosin ATPase reaction times of Dubowitz and Brooke (1973) were modified as

follows: pH 4.2 (2.5 min and 75 min), pH 4.6 (5 min and 40 min), and pH 9.4 (15 min and 5 min) preincubation and incubation times respectively. All sections were cut and stained on the same day to avoid any possible loss of enzyme activity.

With the myosin ATPase reaction, two extrafusal fiber types could be clearly discerned. Myosin ATPase staining of serially sectioned myofibers was compared at acid and alkaline preincubation conditions to check for reversability of staining. Intrafusal fibers were typed according to the bag₁, bag₂, and chain classifications of Ovalle and Smith (1972). The histochemical profile of individual intrafusal fibers was determined by examining serial sections cut along their entire length. Selected transverse profiles were photographed using a Leitz Orthoplan photomicroscope equipped with brightfield optics and a tungsten light source.

Extrafusal Fiber Morphometry

Transverse sections cut through the midbelly region of each tenuissimus muscle were examined with a Leitz bright-field light microscope, fitted with a camera lucida drawing attachment. Entire muscle cross-sections were projected onto the digitizing pad of a Zeiss Mop 3 Image Analyzer, and the outline of each myofiber was then traced. The magnification for tracing was 400x. Means were calculated for the number, cross-sectional area, and maximal diameter of myofibers belonging to each fiber-type category as revealed by the myosin ATPase reaction.

Muscle Spindle Quantitation

Muscle spindles and extracapsular intrafusal fibers were located by light microscopy at a magnification of 400x. With the aid of the camera lucida drawing attachment, the location of each receptor was marked on a replica sketch of the entire muscle cross-section. This

procedure was repeated at 100 μm intervals and the length of each receptor was approximated by counting the number of sections in which intrafusal fibers were seen and then multiplying by a factor of ten.

The total number of muscle spindles per muscle was counted and the muscle spindle index (number of muscle spindles per gram of muscle weight) was then calculated. The number of intrafusal fibers in each muscle spindle was also noted. A diagrammatic longitudinal reconstruction of the muscle spindle distribution throughout one entire tenuissimus muscle was also made from the serial tracings.

Fluorescence Microscopy

The tenuissimus from one adult, male hamster was used to determine the distribution of filamentous actin by fluorescence microscopy in the intrafusal fibers. The animal was killed with an overdose of chloroform and the left tenuissimus was quickly exposed and excised. The resting length of the muscle was maintained by pinning it through its tendons to dental wax and then fixing it by immersion in a solution of 3% paraformaldehyde in phosphate-buffered saline (PBS) (150mM NaCl, 5mM KCl, 3.2mM Na_2HPO_4 , 0.8mM KH_2PO_4 , adjusted to pH 7.3 with 0.1N NaOH) for 15 min at room temperature. The muscle was then rinsed several times in PBS. Under a dissecting microscope equipped with darkfield illumination at a working magnification of 40-50x, two muscle spindles were located and gently teased away from the surrounding extrafusal fibers using fine tungsten needles (A-M Systems, Everett, WA). Isolated spindles were placed on polylysine-coated slides, immersed in acetone cooled to -20°C with liquid N_2 for 5 min, and then air-dried for 30 min. Samples were rehydrated for 10 min with PBS and then exposed, at room temperature, to a solution of PBS and $1.65 \times 10^{-6}\text{M}$ 7-nitrobenz-2-oxa-1,3-diazole (NBD)-phalloidin (Molecular Probes, Eugene, OR). Following three rinses in PBS (10 min each), whole spindle preparations were mounted under glass

coverslips with a mixture (by volume) of 50% glycerol and 50% PBS containing 0.02% sodium azide. Spindles were examined with a Zeiss photomicroscope III fitted with filters used to detect fluorescein isothiocyanate. Fluorescence was recorded on Kodak TMax 400 (35 mm) black and white print film (400 ASA).

OBSERVATIONS

General Morphology

The tenuissimus of the hamster appeared as a long and attenuated muscle that weighed, on average, 37 ± 5.6 mg. When viewed in cross-section by light microscopy, the oval-shaped profile of the muscle was clearly seen, outlined by a dense blanket of epimysial connective tissue (Fig. 1). At certain sites, branches of the epimysial coat penetrated the interior of the muscle to separate a closely packed array of extrafusal muscle fibers into pleomorphic fascicles (Fig. 1). The average number of extrafusal fibers within each muscle was 236 ± 14.4 ($n = 5$). A prominent arterial and venous blood supply was located centrally within the muscle along its entire axial length (Fig. 1). In addition, the main intramuscular nerve trunk was often seen travelling in close association with these blood vessels.

Fiber Type Distribution

The histochemical profiles of extrafusal fibers from serial-sections of the tenuissimus are illustrated in Figures 5-7. Staining of all extrafusal fibers was moderate and uniform in sections treated to detect oxidative enzyme activity using the NADH-TR reaction (Fig. 7). In sections treated to detect myosin ATPase activity, however, two extrafusal fiber types were clearly discerned on the basis of their staining intensities (Figs. 5, 6). At pH 4.2 (Fig. 5), darkly-staining fibers were presumed to be of the type I (slow-twitch) variety and pale-staining fibers were presumed to be of the type IIA (fast-twitch) variety. Serial sections of the same extrafusal fibers preincubated at pH 9.4 (Fig. 6) showed a complete reversal of these staining properties.

Morphometry

Mean fiber-type distribution, expressed as a percentage of the total extrafusal fiber number, showed that the tenuissimus consists of 51% type I fibers and 49% type IIA fibers.

Both of these fiber types were distributed homogeneously throughout entire muscle cross-sections. Type I myofibers had a mean maximal diameter of $35.9 \pm 2.8 \mu\text{m}$ and a mean cross-sectional area of $694.5 \pm 75.1 \mu\text{m}^2$. Fibers exhibiting type IIA staining characteristics had a mean maximal diameter of $38.3 \pm 3.6 \mu\text{m}$ and a mean cross-sectional area of $720.8 \pm 95.7 \mu\text{m}^2$. Overall myofiber cross-sectional area was $707.6 \pm 85.4 \mu\text{m}^2$ with a mean diameter of $37.1 \pm 3.2 \mu\text{m}$.

Muscle Spindle Morphology

The light microscopic appearance of muscle spindles observed in this study was similar to that described for other species (see reviews by Boyd and Smith, 1984; Barker and Banks, 1986). Spindles were readily distinguished in serial-transverse sections by their prominent capsular investment (Figs. 2, 3). Each receptor was embedded within a network of perimysial and endomysial connective tissue, and all were situated parallel to the surrounding extrafusal fibers (Figs. 2, 3). Small blood vessels and branches from the main intramuscular nerve trunk were frequently situated in close apposition to the external aspect of each receptor (Fig. 2).

Most spindles contained four intrafusal fibers, two large-diameter bag fibers and two small-diameter chain fibers (Fig. 2). Bag fibers usually extended well beyond the limits of the capsular sleeve, while the chain fibers were confined to intracapsular regions. In the equatorial and juxtaequatorial regions, the intrafusal fibers were encased by a delicate inner capsule, separating them from the surrounding periaxial space (Fig. 3). An amorphous and flocculent extracellular material was occasionally seen in the periaxial space, especially in equatorial regions (Fig. 3).

Tandem muscle spindles were consistently encountered in each muscle examined, with an average of 2 ± 0.7 per muscle. For analytical purposes, each of the two capsular units forming the tandem spindle was considered as a separate entity. Tandem spindle units were

formed by two separate muscle spindles positioned side-by-side but offset slightly in the longitudinal plane. In the region of overlap, the capsular investments of the two receptors usually fused to form one large outer spindle capsule, enclosing two separate sets of intrafusal fibers within a common periaxial space (Fig. 3). In equatorial and juxtaequatorial regions, each set of intrafusal fibers was usually surrounded by its own inner capsular sleeve (Fig. 3).

Spindle Quantitation and Distribution

Quantitative data for the muscle spindle population of five tenuissimus muscles is summarized in Table I. The distribution and individual lengths of all muscle spindles in a single tenuissimus muscle are shown diagrammatically in Figure 4. Spindles were most often situated in close proximity to the main intramuscular nerve. Spindle density was greatest in the central portion of the muscle where adjacent spindles frequently overlapped. The density of spindles was slightly less near the muscle origin, and very few spindles were located near the muscle insertion (Fig. 4).

The total number of spindles in each tenuissimus muscle was tabulated. Spindle populations ranged between 16 and 20 per muscle with an average of 18.4 ± 0.7 . The muscle spindle index, defined as the total number of spindles in a given muscle expressed per gram of muscle weight, was found to be 502.7. Muscle spindle lengths, including the extracapsular polar regions, averaged 7.5 ± 0.4 mm with a range of 4.7 - 12.2 mm. The longest spindles were usually found in the midbelly region of each muscle.

Spindle Histochemistry

Three intrafusal fiber types were clearly distinguished in all spindles using the myosin ATPase reaction at acid (pH 4.2) and alkaline (pH 9.4) preincubations (Ovalle and Smith, 1972). When stained under acid conditions, bag₁ fibers were moderately stained, bag₂ fibers were darkly stained and chain fibers were lightly stained (Fig. 5). Under alkaline conditions,

bag₂ fibers were darkly stained as were chain fibers, and only the bag₁ fibers stained lightly (Fig. 6). Thus, only the bag₂ fibers exhibited stability under both acid and alkaline conditions. The chain fibers exhibited a complete reversal of their staining properties under the two pH conditions, resembling the staining reversal of the surrounding type IIA extrafusal fibers (Figs. 5, 6).

Regional variations in the staining profiles of the three intrafusal fiber types were observed along the axial length of individual spindles. These variations are summarized diagrammatically in Figure 8. Under acid preincubation conditions, bag₁ fibers stained darkly in the extracapsular regions, moderately in the polar and juxtaequatorial regions, and lightly in the equatorial region. Under alkaline conditions, the bag₁ fiber stained lightly throughout its length. Bag₂ fibers stained darkly under both acid and alkaline conditions throughout their lengths, except in the equatorial region where very little staining was observed. Similarly, chain fibers showed a consistent reversal of staining along their lengths, except in the equatorial regions where they stained lightly.

All three intrafusal fiber types demonstrated considerable regional variability in the pattern and intensity of staining along their lengths when treated to detect NADH-TR activity (Figs. 7, 9). These regional changes occurred independently of regional variations in the intensity of myosin ATPase staining. In general, the NADH-TR reaction was found to be less suitable for typing of intrafusal fibers than were the two ATPase reactions.

In the equatorial zone, all three intrafusal fiber types exhibited a high degree of NADH-TR activity in their subsarcolemmal regions and in areas intervening between their multiple nuclei. Chain fibers exhibited high oxidative enzyme activity throughout their lengths except for their polar ends where they displayed only moderate NADH-TR activity. Bag₂ fibers stained only moderately in all regions outside of the equatorial zone. The bag₁ fibers displayed the most variability in terms of regional staining intensity. Oxidative enzyme activity was

only moderate in the juxtaequatorial regions but became progressively more intense in the polar regions. In the extracapsular regions, however, staining intensity was again only moderate. The staining profiles of the three intrafusal fiber types for NADH-TR activity are shown diagrammatically in Figure 9.

Fluorescent Staining of Actin in Isolated Spindles

Spindles could be isolated by dissection as individual, intact units or as tandem spindle units (Fig. 10). When viewed under darkfield illumination the spindle capsule could be seen as a slender and semitransparent fusiform structure (Fig. 10). Nerve bundles could be seen associated with the capsule in the juxtaequatorial region. Within the capsule, a thin intrafusal-fiber bundle could be seen coursing along the axial length of the spindle (Fig. 10).

When treated with NBD-phalloidin, isolated spindles stained intensely for F-actin. Figure 11 shows four intrafusal fibers from an isolated spindle stained with NBD-phalloidin and viewed by fluorescence in the juxtaequatorial region. On the basis of fiber diameter, the two largest intrafusal fibers (14.7 μm and 10.7 μm) were considered to be bag fibers. In contrast, the two smaller intrafusal fibers (9.4 μm and 7.6 μm) were interpreted as chain fibers. F-actin banding-patterns were prominently outlined along the length of each fiber. The nature of the banding pattern was clearly different amongst the four fibers. One fiber, considered to be a bag fiber, had prominent, wide bands separated by distinct non-staining regions. Each band measured approximately 2.2 μm in width. The bands of the second bag fiber appeared much finer and were less clearly defined. The bands of the two chain fibers were similar to those of the second bag fiber but the regions between bands appeared slightly more pronounced. A much higher level of contrast existed between staining and non-staining regions of one chain fiber. The second chain fiber appeared to have very thin and faint bands of stain interspersed in regular fashion between the more pronounced bands.

DISCUSSION

The light microscopic features and the morphometric parameters of the hamster tenuissimus and its associated muscle spindles have been documented for the first time in this study. Unlike its counterpart in the cat which contains between 700 and 1300 extrafusal fibers (Boyd, 1956), the hamster tenuissimus contains an average of 236 extrafusal fibers. While three extrafusal fiber types appear to exist in the cat tenuissimus (Lev-Tov et al., 1988), the present report has demonstrated that only two extrafusal fiber types can be detected histochemically in the hamster tenuissimus. The fibers are distributed evenly and homogeneously throughout the entire muscle cross-section. Type I fibers account for 51% of the extrafusal fiber population and type IIA fibers constitute the other 49%. In the cat tenuissimus, type I fibers account for only 25%, while type IIA fibers make up 16% and type IIB fibers make up 36% of the total extrafusal fiber population (Lev-Tov et al., 1988).

Despite the differences in total number and fiber-type distribution between the cat and hamster tenuissimus, the myofibers of the two muscles have dimensions that are surprisingly similar. Boyd (1956) reported that extrafusal fibers in the cat tenuissimus have a mean diameter of 30-35 μm depending on location within the muscle. Fiber diameters in the hamster tenuissimus averaged 37.1 μm . Lev-Tov et al. (1988) reported that the mean cross-sectional area of extrafusal fibers in the cat tenuissimus was 717 μm^2 . The cross-sectional areas in the hamster reported here are only slightly smaller at 708 μm^2 .

Direct comparisons between the two muscles and with other muscle types must be looked upon with some caution because of the complex internal architecture of the tenuissimus. This muscle in the cat is considered to be "parallel-fibered," made up of short extrafusal fibers with tapered ends (Lev-Tov et al., 1988). In addition, these fibers in the cat originate and insert in serial arrangements within the muscle belly itself (Loeb et al., 1987). Any

cross-sections cut through their tapered ends would reveal small-diameter profiles that may not accurately reflect true myofiber dimensions.

Muscle Spindle Density

Muscle spindle density is usually expressed in terms of the number of muscle spindles per gram of mean muscle weight and is commonly referred to as the *muscle spindle index* (Barker, 1974). The number of spindles in a muscle is usually determined in part by muscle function (Voss, 1937; Cooper, 1960; Barker, 1974; Kennedy et al., 1980; Barker and Banks, 1986). In general, high spindle densities characterize muscles that initiate fine skilled movements, maintain posture, possess slow contractile properties, or have many of their spindle units linked together in tandem or in compound arrangements (Barker and Chin, 1960; Swett and Eldred, 1960; Yellin, 1969a; Peck et al., 1984; Barker and Banks, 1986).

The extremely high spindle density in the tenuissimus, coupled with a relatively low number of extrafusal fibers, is suggestive of a possible role in sensory feedback. Furthermore, given its anatomical arrangement in the hindlimb, the tenuissimus may in fact form part of a "parallel muscle combination" (PMC) (Peck et al., 1984) with the larger, more powerful biceps femoris muscle. A PMC is defined as two muscles that act across a joint in parallel with one another (Peck et al., 1984). One member of the pair is small and presumably functions to provide fine adjustments in movement, while the larger member of the pair may be responsible for gross movement. Peck and co-workers (1984) have shown that the smaller members of PMC's have spindle densities that are three times greater than the spindle densities of their larger counterparts. These workers have concluded that the smaller PMC members function as "kinesiological monitors" generating important proprioceptive feedback to the central nervous system. It is tempting to speculate that the tenuissimus functions in such a manner although the muscle spindle index for the biceps femoris muscle of the hamster has not as yet been determined. A spindle index of 502.7 makes the tenuissimus of

the hamster one of the most densely-populated muscles yet studied. Previously, the highest spindle index recorded for mammalian muscles was 328 for the cat intervertebral centrotransverse muscle (Bakker and Richmond, 1982). In addition, the delicacy, small cross-sectional area, and minimal force-output capacity of the tenuissimus, preclude any significant contribution to overall movement about the hip and knee (Lev-Tov et al., 1988).

Spindle Histochemistry

In the hamster tenuissimus, three intrafusal fiber types could be distinguished on the basis of myosin ATPase staining characteristics. Moreover, regional variations in staining intensity were observed, similar to those noted in other muscles of the mouse (Johnson and Ovalle, 1986), rat (Soukup, 1976; Banks et. al., 1977; Khan and Soukup, 1979), cat (Banks et al., 1977; Bakker and Richmond, 1981; Kucera, 1981), monkey (Ovalle and Smith, 1972), and human (Kucera and Dorvini-Zis, 1979). As in other mammalian species, bag₁ fibers exhibited low alkaline activity but were acid-stable. Bag₂ fibers were both acid and alkaline-stable, and chain fibers were acid-labile but exhibited high alkaline activity.

When compared with intrafusal fibers of the cat tenuissimus, intrafusal fibers of the hamster showed regional variations that were slightly different. Kucera (1981) reported that the degree of alkaline stability of bag₁ and bag₂ fibers varies from capsular to polar regions. Bag₁ fibers in the cat are alkaline-labile in the equatorial and polar zones, but exhibit moderate activity in juxtaequatorial regions. In contrast, bag₁ fibers in the hamster tenuissimus appeared alkaline-labile throughout their entire lengths. Bag₂ fibers in the cat display high alkaline stability in the equatorial region but this activity diminishes towards the poles. Bag₂ fibers in the hamster exhibited high alkaline activity throughout their lengths. The staining profiles of both fiber types under acid preincubation conditions were similar. It is noteworthy that chain fibers in both species share identical acid/alkaline staining properties.

It is interesting to note that regional histochemical variations along the lengths of extrafusal fibers are not characteristic of mammalian muscles (Farrell and Fedde, 1969; Pette et al., 1980; Nemeth et al., 1981). Why then do intrafusal fibers exhibit such staining variations? Yellin (1969b) and Milburn (1973) suggested that the histoenzymatic differences that characterize intrafusal fibers are determined by their fusimotor innervation. However, Zelená and Soukup (1973, 1974) have shown that rat muscle spindles develop and differentiate to form their normal histochemical profiles despite irreversible deprivation of motor innervation at birth. Zelená and Soukup (1973, 1974) have suggested that the sensory innervation of spindles is of primary importance in the determination of the basic morphological and histoenzymatic properties of the intrafusal fibers. Similarly, Kucera (1981) found no correlation between regional enzymatic profiles of intrafusal fibers and the pattern of their motor innervation. Kucera (1981) concluded that the histochemical properties of intrafusal fibers are regulated in a manner different from that of the surrounding extrafusal muscle fibers.

It has also been shown that the three types of mammalian intrafusal fibers contain different isoforms of myosin in capsular (Pierobon-Bormioli et al., 1980; te Kronnie et al., 1981; Rowlerson et al., 1985; Maier et al., 1988) and extracapsular polar regions (Kucera and Walro, 1989). In addition, it has been reported that, like myosin ATPase staining, myosin heavy chain expression varies along the lengths of intrafusal fibers but is uniform along the length of normal extrafusal fibers (Kucera and Walro, 1989). These workers showed that strong binding of avian slow-tonic and avian neonatal antibodies was usually restricted to the intracapsular regions of the intrafusal fibers. In contrast, the extracapsular regions of these fibers displayed strong mammalian slow-twitch and mammalian fast-twitch antibody reactivity (Kucera and Walro, 1989). In addition, Kucera and Walro (1989) have shown that there is a relationship between myosin ATPase activity and the expression of myosin heavy chain isoforms in the extracapsular regions of intrafusal fibers but not in the intracapsular

regions. A similar relationship appears to hold true for extrafusal fibers (Staron and Pette, 1986).

In this study, the presence and distribution of F-actin within intrafusal fibers of the hamster were demonstrated using the fluorescent probe NBD-phalloidin. The different banding patterns noted along individual muscle fibers may be a reflection of their different mechanical and ultrastructural properties. At the ultrastructural level, it has been shown that a distinct and single M line is present along the entire length of chain fibers, and in all regions of bag₂ fibers except for the equator (Banks et al., 1977). A distinct M line is usually absent in all regions of bag₁ fibers except for extracapsular regions, although a faint double-M line is sometimes present (Banks et al., 1977). In addition, the bag₁ fibers have thicker Z bands and the arrangement of contractile proteins is such that there is a great deal of contrast between the A and I bands when examined longitudinally by transmission electron microscopy. Such features are not characteristic of either bag₂ or chain fibers (Barker, 1974; Boyd and Smith, 1984).

In conclusion, the hamster tenuissimus is a hindlimb muscle that contains a mixed population of type I and type IIA extrafusal fibers. It also contains an extremely dense population of muscle spindles indicating that this muscle may play a critical role in hindlimb proprioception. The combination of high spindle number and low extrafusal fiber number makes this muscle ideal for the microdissection and isolation of these receptors for further morphological analysis.

CHAPTER 2

ELECTRON MICROSCOPY OF MUSCLE SPINDLES IN THE HAMSTER TENUISSIMUS

ABSTRACT

Muscle spindles in the hamster tenuissimus were studied by transmission (TEM), conventional scanning (SEM) and high resolution scanning (HRSEM) electron microscopy. For SEM, muscles were first fixed in 2.5% buffered glutaraldehyde. Spindles were then isolated with a dissecting microscope under darkfield illumination and postfixed in 1.0% OsO₄. Some spindles were treated with 8N HCl at 60° C to expose intrafusal fiber surfaces once the outer capsule was mechanically disrupted. Preparation for HRSEM included aldehyde/osmium fixation and freeze-cleavage in liquid N₂. The cytosol was also selectively extracted by immersion in 0.1% OsO₄ for varying times. In these specimens, the capsular sleeve showed a multilayered pattern of vesicle-laden cells with variant surface topography in different regions, including filopodia and small bristle-like surface-projections. An interlacing network of collagen fibrils intervened between capsular lamellae. Within the spindles, sensory and fusimotor nerve endings closely adhered to the outer surfaces of intrafusal fibers. By TEM and HRSEM, sensory terminals appeared crescent-shaped and were enveloped by external laminae. Each profile contained a plethora of elongated mitochondria that ran parallel to the longitudinal axis. Multiple adhesion sites between the sensory nerve membrane and the underlying sarcolemma of the intrafusal fiber were also observed. Fusimotor nerve endings were covered externally by processes of Schwann cells and their axoplasm was filled with many organelles and synaptic vesicles. Dilated cisternae of the sarcoplasmic reticulum and numerous mitochondria were, in addition, observed below the postjunctional sarcolemma at the neuromuscular interface. The methodology used in this study provides a novel view of the exquisite three-dimensional architecture of this neuromuscular receptor.

INTRODUCTION

Since the work of Sherrington (1894) and Ruffini (1898), the specialized sensory stretch-receptors of skeletal muscle known as muscle spindles have been the subject of intense physiological and morphological inquiry. Their intricate connections with the central nervous system have motivated investigators to further elucidate details of their morphological makeup to better understand their complex functions.

Our current understanding of muscle spindle ultrastructure was initiated by a series of morphological studies conducted in the 1960's (Merrillees, 1960; Katz, 1961; Karlsson et al., 1966; Landon, 1966; Adal, 1969; Corjava et al., 1969) and early 1970's (Banker and Girvin, 1971; Ovalle, 1971, 1972a, b; Smith and Ovalle, 1972; James and Meek, 1973; Barker, 1974). Utilizing the resolving capabilities of the conventional transmission electron microscope (TEM), these authors provided detailed and descriptive accounts of the fine structure of spindles as seen in two dimensions. In more recent times serial-reconstruction techniques have been utilized to illustrate the three-dimensional organization of sensory (Scalzi and Price, 1971; Kennedy et al., 1975; Banks, et al., 1982; Banks, 1986) and fusimotor (Banks et al., 1978; Banks, 1981b; Arbuthnott et al., 1982; Kucera, 1982c) nerve endings in spindles from several species. Further illustration of the three-dimensional morphology of sensory terminals has been provided by Quick (1984) using freeze-fracture electron microscopy.

Only one group has utilized the favorable resolving capabilities of the conventional scanning electron microscope (SEM) to explore the muscle spindle's internal surface-morphology (Schröder et al., 1988, 1989). These workers employed a modified version of the HCl-collagenase digestion method originally devised by Evan et al. (1976) to prepare isolated spindles for SEM evaluation. With this new approach, details of the three-dimensional arrangement of intrafusal fibers and their associated nerve endings, along with elements of the

capsular sleeve, were revealed in unique fashion.

The development of high resolution scanning electron microscopy (HRSEM) by Tanaka (1972) and Tanaka and Mitsushima (1984), and its modification and further improvement by Hollenberg and co-workers (1989) are noteworthy. The innovative specimen preparation techniques of this methodology along with advances in modern SEM technology provide an opportunity to observe internal cellular and tissue ultrastructure, not only in three dimensions, but at a resolution approaching that of conventional TEM (Hollenberg and Lea, 1988).

The tenuissimus in the cat has been used extensively in studies of muscle spindle physiology because of the unique arrangement and relatively high content of these sensory receptors (Boyd, 1956). For these reasons, this muscle has also been chosen for TEM studies of muscle spindle ultrastructure (Adal, 1969; Scalzi and Price, 1971; Butler, 1979, 1980). The present study was designed to examine the three-dimensional morphology of muscle spindles from the tenuissimus muscle of golden syrian hamsters using both conventional and high resolution SEM. The tenuissimus in the hamster was chosen for use in this study because its numerous spindles are not only easily accessible but, like those in the tenuissimus of the cat, they are also arranged in-series along its entire length with a relative paucity of surrounding extrafusar fibers (Desaki and Uehara, 1983). A preliminary report of a portion of this work has been published elsewhere (Patten and Ovalle, 1990), and a paper has recently been accepted for publication (Patten and Ovalle, 1991).

METHODS

Eleven tenuissimus muscles of normal, adult male golden syrian hamsters (*mesocricetus auratus*) were used. Animals were kindly provided by Dr. R. Shah in the Department of Oral Biology at the University of British Columbia, from breeding pairs originally obtained from Simonson's Laboratories, Gilroy, CA. A total of 19 spindles from 7 animals were examined; 2 were prepared for TEM, 10 were prepared for conventional SEM and 7 were prepared for high resolution SEM. Animals were first killed with an overdose of chloroform, and tenuissimus muscles were then immediately exposed by dissection.

TEM

Muscles were first fixed *in situ* for 15 min by the dropwise application of a mixture of 2.5% glutaraldehyde and 1% paraformaldehyde in 0.1M phosphate buffer. Whole muscles were then excised, pinned to dental wax at a length approximating resting conditions, and immersed in a pool of fresh fixative for 15 min. Each muscle was then cut into small segments, no longer than 3 mm, placed in fixative for an additional 2 hrs at room temperature, and washed in repeated changes of buffer. Muscle segments were postfixed in 1% OsO₄ in 0.1M phosphate buffer for 1 hr, rinsed several times in distilled water and stained *en bloc* with 1% aqueous uranyl acetate for 1hr. Following several rinses in distilled water, tissue samples were dehydrated in ascending grades of ethanol and propylene oxide, and infiltrated overnight in a mixture of Epon 812 resin (Electron Microscopy Services, Port Washington, PA) and propylene oxide. The following day, specimens were infiltrated with 100% resin, placed in specimen molds, and polymerized for 48 hrs at 60° C. To localize spindles within the blocks, thick sections (1 µm) were cut with glass knives on a Reichert OMU-3 ultramicrotome and stained with 1% aqueous toluidine blue. Once a spindle was located, thin sections were cut with a diamond knife, placed on copper grids, stained with 4% aqueous uranyl acetate and Reynold's

(1963) lead citrate and examined in a Philips 300 transmission electron microscope operated at 60 kV.

Conventional SEM

Muscles were first fixed *in situ* for 15 min at room temperature by the dropwise application of a mixture of 2.5% glutaraldehyde in 0.1M phosphate buffer (pH 7.2). After excision, whole muscles were pinned to dental wax at a length approximating resting conditions, immersed in fresh fixative for an additional 2 hr and washed in repeated changes of buffer. Under a dissecting microscope equipped with darkfield illumination at a magnification of 40-50x, individual spindles were pinpointed and gently teased away from the surrounding extrafusal fibers using fine tungsten needles (A-M Systems, Everett, WA). Isolated spindles were postfixed in 1% OsO₄ in 0.1M phosphate buffer for 1 hr and washed again in repeated changes of buffer at room temperature. Some spindles were treated with 8N HCl at 60° C for 30-60 min (Desaki and Uehara, 1981) to more clearly expose the outer surfaces of intrafusal fibers and associated internal structures. Specimens were rinsed in distilled water, dehydrated in a graded series of ethanols, dried by a critical point method utilizing Freon TF as an intermediate fluid and liquid CO₂ as a transitional fluid (Vesely and Boyde, 1973), and then mounted on aluminum stubs with colloidal graphite paint. Each specimen was sputter coated with gold in an Edwards E12E vacuum evaporator set at 1.2 kV and 5 mA for 5 min, and examined in a Cambridge S4 Stereoscan SEM at an accelerating voltage of 20 kV.

High Resolution SEM

Whole muscles were first pinned under moderate stretch through their tendons to dental wax and then rapidly fixed by immersion in a mixture of 0.5% glutaraldehyde and 0.5% paraformaldehyde in 0.07M phosphate buffer (pH 7.2) for 15-45 min at room temperature. Following repeated rinses in buffer, muscles were cut with a razor blade into small pieces, no more than 3 mm in length, and postfixed in 1% OsO₄ in 0.07M phosphate buffer for 90 min.

Tissue processing was undertaken according to the method of Tanaka and Mitsushima (1984) modified by Hollenberg and co-workers (1989). Specimens were washed in buffer, placed in 25% aqueous dimethylsulfoxide (DMSO) for 30 min, and then in 50% DMSO for 30 min. They were then quick-frozen in liquid Freon 22 cooled with liquid N₂ at -196° C. Frozen samples were transferred to a brass well filled with liquid N₂ and cracked open using a hammer and a pre-cooled razor blade. Cleaved specimens were thawed in 50% aqueous DMSO for 5-10 sec at room temperature, postfixed in 1% phosphate buffered OsO₄ for 1 hr and rinsed in repeated changes of buffer. Certain cellular elements, including the cytosol, were then selectively extracted by incubating tissue samples in phosphate buffered 0.1% OsO₄ for 1-3 days at room temperature. After the desired extraction was achieved, samples were rinsed in buffer, placed in 1% aqueous tannic acid for 1 hr, rinsed in buffer, placed in 1% OsO₄ for 1 hr, and rinsed again in buffer. Dehydration was accomplished through a graded ethanol series, and specimens were dried by a critical point method employing absolute ethanol as an intermediate fluid and liquid CO₂ as a transitional fluid (Lea and Ramjohn, 1980). Dried samples were mounted on aluminum pin stubs with colloidal graphite paint, coated with a thin layer of gold in a Polaron SEM Coating System set at 2.4 kV and 20 mA for 30 sec, and examined in a Hitachi S-570 SEM at an accelerating voltage of 20 kV and a working distance of 0 to -4 mm. Stereo pairs were obtained by tilting specimens 10° (125 steradians) and photographing the surface of a high resolution cathode ray tube with Polaroid 55 (4x5 inch) positive-negative sheet film (ASA 50).

OBSERVATIONS

General Morphology

By both conventional and high resolution SEM, spindles could be visualized in three dimensions and in considerable detail. When viewed in cross-section and at low magnification, they could be seen in their entirety (Figs. 12, 13). In the equatorial region (Fig. 12), three to four intrafusal fibers were typically encountered with cross-sectional diameters ranging between 7 and 13 μm . All intrafusal fibers were closely enveloped by a delicate inner capsule. The outer surface of this axial sheath was coated by an interlacing meshwork of connective-tissue fibrils. More externally, a prominent periaxial space separated the inner capsule from the more conspicuous outer capsule (Figs. 12, 13). The outer capsule itself appeared multilayered, and profiles of nerve axons and capillaries were at times observed to be embedded within the lamellae (Fig. 12).

Treatment of isolated spindles with 8N HCl resulted in a variable degree of dissolution of connective-tissue and capsular elements. On occasion, portions of both the outer and the inner capsules were removed revealing the striated surfaces of the intrafusal fibers (Fig. 14). In these preparations a highly registered sarcomere-banding pattern, with a repeat of approximately 1 μm , was observed. Numerous nerve-fiber branches occupied portions of the adjacent periaxial space, and they were aligned in parallel with the intrafusal fibers (Fig. 14).

Outer Capsule

When treated with 8N HCl, pericapsular connective tissue was usually completely removed unveiling the smooth surfaces of outer capsule cells (Figs. 14, 15). Three sites of nerve-fiber entry were usually encountered along the length of the capsule; one in the equatorial region and one in each of the juxtaequatorial regions. At these sites, a direct continuity between the perineurial sheath of the nerve fascicle entering the spindle and the

outer capsule itself, was clearly seen (Fig. 15). By SEM, perineurial epithelial cells of both the sheath and the outer capsule were arranged in a contiguous fashion, and the cells appeared flattened and pleomorphic. Capillaries were observed in close association with individual nerve fascicles (Fig. 15) or with the outer surface of the capsule itself (Fig. 13). While these vessels were composed of a single layer of endothelial cells, it was not possible to determine whether they possessed fenestrations or whether they were linked together by tight junctions.

A closer inspection of the capsule in the equatorial and juxtaequatorial regions revealed a complex syncytium of elongated, attenuated cells with layers of connective-tissue fibrils occupying the spaces between adjacent lamellae. The number of cell layers varied from region to region within each spindle, and was usually greatest in the equatorial zone (Fig. 12). The axis of orientation of the interlamellar collagen fibrils differed from layer to layer with some aligned in longitudinal fashion and others arranged in a circumferential or oblique manner (Figs. 16, 17). A dense aggregation of larger-diameter collagen fibrils, measuring 100 nm in diameter, formed a sheath-like encasement around the outer limits of the entire capsular sleeve (Figs. 12, 16).

When capsular cells were cleaved open, profiles of cytoplasmic organelles including mitochondria, rough-surfaced endoplasmic reticulum, and numerous transcytotic vesicles were scattered within individual cells (Fig. 16). Cytoplasmic vesicles were distributed evenly throughout the perineurial cells of the capsular wall and were uniform in size and spherical in shape, measuring 60-80 nm in diameter.

A striking feature of the capsular cells was their variant and somewhat peculiar surface morphology (Figs. 17, 18). In the outermost layers of the capsule, cells typically appeared smooth-surfaced and contiguous. In the innermost layers, however, cells exhibited a flattened and unevenly fenestrated appearance with tenuous cytoplasmic processes resembling filopodia (Fig. 17). A scattered array of underlying collagen fibrils occupied the fenestrated spaces

formed by the numerous filopodia. In addition, many small and randomly-arranged surface-projections studded the external surfaces of these cells in a bristle-like fashion (Figs. 17, 18). The sizes of these surface specializations varied from cell to cell with most being 75-125 nm in length and 25-50 nm in diameter.

Inner Capsule

Cells of the inner capsule formed a delicate axial sheath around intrafusal fibers in the equatorial and juxtaequatorial regions (Fig. 19). Each cell contained a large, ovoid-shaped nucleus housed within a prominent cell soma (Fig. 20). Moreover, dense masses of chromatin usually occupied the regions directly under the nuclear envelope (Fig. 20). Thin and flattened cytoplasmic processes emanated from the cell body of each inner capsule cell. These cellular extensions were often branched, and formed a loose sleeve around individual intrafusal fibers in the sensory region (Fig. 19). Within the axial compartment, subjacent to the inner capsule, a prominent external lamina, composed of an interwoven meshwork of extracellular fibrils, formed a tight blanket around individual intrafusal fibers and their associated sensory nerve endings (Fig. 19).

Within cells of the inner capsule, scattered profiles of rod-shaped mitochondria and dilated cisternae of rough-surfaced endoplasmic reticulum were prominent cytoplasmic features (Figs. 19, 20). On some occasions, groups of mitochondria were stacked in-parallel along the longitudinal axis of the spindle itself (Fig. 19). In addition, large and well-developed perinuclear Golgi complexes were typically surrounded by numerous cytoplasmic vesicles and vacuoles, implicating these cells in metabolic and protein synthetic activities (Fig. 20).

Fusimotor Nerve Endings

Fusimotor nerve endings on intrafusal fibers were observed in the juxtaequatorial and polar regions of spindles prepared for HRSEM. Figure 21 shows details of a motor nerve

terminal in the juxtaequatorial region that measures 3 μm in width, and is closely apposed to an underlying intrafusal fiber. Motor nerve terminals were typically seen as punctate elevations above the muscle fiber surface (Fig. 13). Long and slender processes of associated Schwann cells formed an external cap around the axon terminal. They extended beyond the limits of the nerve terminal to partially blanket the surface of the underlying intrafusal fiber (Fig. 21).

Within the motor nerve terminal, mitochondria of various shapes and sizes intermingled with lysosomes. Numerous spherical-shaped synaptic vesicles, 50-70 nm in diameter, were also concentrated in the axoplasm. In addition, a narrow synaptic cleft, 20-40 nm in width, separated the neuronal membrane from the underlying sarcolemma (Fig. 21). The postjunctional sarcoplasm contained many tightly-packed mitochondria arranged in row-like fashion. The rounded appearance of these organelles may have been the result of cleavage of the muscle fiber in the transverse plane (Fig. 21).

On either side of the junction, dilated cisternae of the sarcoplasmic reticulum (SR) were often seen in close apposition to the inner surface of the sarcolemma (Fig. 21). These spherical-shaped organelles measured 400-800 nm in diameter, and they were also seen closely apposed to an array of tightly-packed mitochondria (Fig. 21). The luminal contents of each of these sarcoplasmic cisternae were presumably extracted by the preparative procedures for HRSEM, revealing the smooth inner surface of their membrane (Fig. 21).

Sensory Nerve Endings

Sensory nerve endings were encountered along the external surfaces of intrafusal fibers in equatorial regions. By conventional SEM they appeared as punctate, bulbous expansions (Fig. 23). In cross-section, nerve terminals appeared crescent-shaped and often formed shallow depressions on intrafusal-fiber surfaces (Figs. 22, 24). Each afferent-terminal

profile contained a plethora of closely-packed and evenly-distributed mitochondria (Figs. 22, 24-27). Variations in the shapes and sizes of these organelles were noted with the majority being elongated and cylindrical, whereas others occasionally took on a flattened and disk-like appearance (Fig. 25). In addition, the longitudinal axes of the majority of these organelles appeared to be oriented in parallel with the long axis of the sensory terminal (Fig. 26). When cleaved open, these mitochondria were seen to possess tightly-packed cristae with an inner matrix that often appeared somewhat granular (Fig. 25).

Other prominent cytoplasmic organelles in the afferent terminals included lysosomes and a varied assortment of membrane-bounded vesicles measuring 70-140 nm in diameter (Figs. 22, 26, 27). In addition, small membrane-bounded tubular profiles in the axoplasm were seen in close association with the neuronal membrane at various points along the nerve-muscle boundary (Fig. 25). These tubular profiles measured 100-200 nm in diameter. At the nerve-muscle interface, the neuronal membrane lay in close apposition to the underlying sarcolemma of the intrafusal fiber with an intervening cleft that measured 30-80 nm wide (Figs. 22, 23, 25, 27). Multiple sites of punctate junctional adhesion appeared to link the two membranes at select regions along this interface (Figs. 25, 27).

Numerous axoplasmic filaments formed a delicate latticework within each sensory terminal, and many were arranged in close association with the mitochondria (Fig. 26). At the outer face of the sensory terminal, axoplasmic filaments also appeared to be anchored in a regular fashion to the inner surface of the cell membrane, giving it a pleated appearance (Fig. 26). In most places, a prominent external lamina was shared by both the intrafusal fiber and its sensory terminals, separating them from the adjacent inner capsular sheath (Figs. 24, 26). Schwann cells and myosatellite cells were notably absent in these regions and sensory cross-terminals, first described by Adal (1969) in the tenuissimus of the cat, were not encountered.

Selective extraction of the closely-packed myofilament lattice at the site of nerve-muscle contact by prolonged exposure to OsO₄ revealed a close relationship between the SR of the intrafusal fiber and the sarcolemma. Entwined tubular elements of the SR, measuring 40-100 nm in diameter, formed an anastomosing network that arose in vertical fashion from within the intrafusal fiber to make contact with the sarcolemma (Fig. 27). At the nerve-muscle interface these tubular profiles could be seen along the undersurface of the sarcolemma and occasionally appeared to be linked to it via small attachment plaques (Fig. 27). Other small and somewhat flattened T-tubular profiles were arranged horizontally, directly below the site of nerve-muscle contact (Fig. 27).

DISCUSSION

In this report, conventional TEM, conventional SEM and the more recently developed technique of HRSEM have been used to visualize both the surface topography and the internal cellular morphology of muscle spindles. Although spindles have been studied extensively by TEM over the past thirty years, there is limited information in the literature about their three-dimensional organization at the fine structural level. Use of the present methodologies has permitted direct observation of the three-dimensional architecture of these unique receptors and has revealed a number of interesting and unusual ultrastructural features.

Outer Capsule

The three-dimensional appearance of the outer capsule, as seen by HRSEM, is consistent with previous studies by TEM. The direct continuity of the spindle capsule with the perineurial sheath of the peripheral nerve supply to the receptor has been noted in the past (Merrillees, 1960; Shantha and Bourne, 1968; Shantha et al., 1968; Corjava et al., 1969, James and Meek, 1973; Ovalle, 1976), and is now demonstrated for the first time by scanning electron microscopy.

Studies by Kennedy and Yoon (1979), Dow and co-workers (1980), and Fukami (1982) have shown that outer capsule cells of muscle spindles, like perineurial epithelial cells of nerve fascicles, form a selective barrier to the passage of exogenous tracers. More recent work (Fukami and Schlesinger, 1989) has shown that this selective permeability is a result of endocytotic and transcytotic activity within individual cells. Our observations correlate well with these results. The myriad of spherical cytoplasmic vesicles seen in cross-sectional views of the outer capsular wall is consistent with some type of regulatory activity occurring in these regions. The spherical nature of these structures also serves to illustrate an advantage offered by HRSEM in evaluating cellular ultrastructure from a three-

dimensional perspective. It is clear from the micrographs in this report (see Figs. 16-18) that the structures are singular and vesicular in nature and are not merely open/closed channels traversing the capsular cell walls. Such transcellular channels have been reported to exist in other cell types such as vascular endothelial cells (Simionescu et al., 1975).

Shantha and co-workers (1968) have shown the capsule to be a metabolically active structure by demonstrating the presence of various oxidative and phosphorylative enzymes. The rich and varied organelle content of capsular cells, including profiles of rough-surfaced endoplasmic reticulum and elements of the Golgi complex, suggests also that these cells may be actively engaged in protein synthetic activity for export. Their main secretory product may in fact be the dense aggregations of collagen and elastic fibrils that are known to occupy the paracellular regions of the receptor (Cooper and Gladden, 1974; Maier and Mayne, 1987). Further involvement in the production of the hyaluronic acid within the periaxial space (Brzezinski, 1961a, b; James, 1971; Fukami, 1982, 1986) is another distinct possibility. Unfortunately, the nature of the periaxial fluid could not be observed in this study, as the methodology employed resulted in its complete extraction from within each spindle.

Perhaps the most intriguing aspect of the outer capsule was the unusual cellular topography observed in its innermost layers. The cells occupying these regions were fenestrated and possessed long and flattened cytoplasmic filopodia extending in all directions. The precise function of these cells is somewhat unclear particularly in light of the role the capsule plays in protecting and regulating the internal microenvironment of the spindle. It may well be that these innermost cells are of less importance than the outermost layers in maintaining the permeability characteristics of the capsule. Indeed, Kennedy and Yoon (1979) have demonstrated that penetration of the exogeneous tracer, horseradish peroxidase, into the periaxial space is halted primarily by cells occupying the outer two to three layers of the equatorial capsule.

Reiss and Noden (1989) have recently published micrographs showing similar cellular topography to the filopodia-laden capsular cells in their SEM study of the developing quail embryo. Their descriptions of the *subvascular plate*, as a developing monolayer of flattened cells with cytoplasmic filopodia, were morphologically similar to the capsular cells seen in the present HRSEM micrographs (see Figs. 17, 18). Reiss and Noden (1989) suggest that the cells of the subvascular plate, which are arranged in close association to developing vascular endothelium, may play a role in the formation of perivascular smooth muscle, paracellular connective tissue, and vascular pericytes. Whether the filopodia-laden cells in the outer capsule play a similar role in vascular maintenance is uncertain although the contribution of the outer capsular cells to a functional blood-muscle spindle barrier has been previously documented (Kennedy and Yoon, 1979; Dow et al., 1980; Fukami, 1982).

An alternative explanation would be to consider these filopodia-laden cells as a less-differentiated subpopulation of cells within the capsule with the potential to form additional capsular lamellae in response to injury or to certain disease processes. The thickening of the outer capsule in diseases such as muscular dystrophy (Ovalle and Dow, 1986) and in response to denervation (Schröder, 1974; Swash and Fox, 1974; Kucera, 1980b) tends to support this notion. Furthermore, given the importance of the capsule in maintaining the integrity of the internal microenvironment of the spindle (Kennedy and Yoon, 1979; Dow et al., 1980; Fukami, 1982, 1986), and its putative role in providing a scaffold for intrafusal fiber regeneration (Rogers and Carlson, 1981), it would make sense for the outer capsule to contain a cell population of this nature.

Bridgman and Eldred (1964) have suggested that the outer spindle capsule functions as a pressure-sensitive organ that is directly responsive to changes in intramuscular pressure brought on by extrafusal fiber contraction. It is tempting to speculate that the specialized subpopulation of capsular cells might somehow provide the outer capsule with some degree of elasticity or even contractility. If these cells were of a contractile nature, they would enable

the capsule to accommodate any changes in length or shape brought on by the contractile shortening of the surrounding extrafusal muscle fibers. In this context, it would be tempting to liken them to myoepithelial cells since cells of the spindle capsule also contain actin and vimentin (Ovalle and Dow, 1988). Further investigation into their structural and functional makeup would be needed, however, before direct comparisons could be made. In the present SEM study, microfilaments were not observed in cells of the spindle capsule. Their presence in these cells, however, has been verified by TEM, consistent with the view that the capsule exhibits contractile properties (Ovalle and Dow, 1988).

The small microvillus-like surface-projections dispersed across the external surfaces of some outer capsule cells is a further observation of intrigue. They have not been described in previous reports of the muscle spindle's outer capsule, although cells comprising its inner capsule have been reported to possess cilia (Ovalle, 1976). While it is doubtful that these surface-specializations are true cilia because of their small size, it is possible that they represent smaller microvilli. The presence of microvilli on cell surfaces is often associated with some type of absorptive or secretory function (Griep and Robbins, 1988). If these surface-specializations are indeed microvilli, their presence would lend further credence to the notion that outer capsule cells actively secrete and maintain components of the paracellular matrix.

Inner Capsule

From a three-dimensional perspective, the inner capsule of the muscle spindle appears as an aggregation of flattened and contiguous cells which branch to form an intimate investment around individual intrafusal fibers and their sensory terminals, isolating them from the equatorial periaxial space. This arrangement has important functional implications as inner capsule cells also contribute to the blood-muscle spindle barrier. Dow et al. (1980) have shown that these cells phagocytose exogeneous tracers that enter the periaxial space. Such

activity presumably protects and maintains the integrity of the axial compartment and prevents foreign substances from gaining access to the intrafusal fibers and their associated sensory nerve endings.

Muscle spindle inner capsule cells have been compared to other specialized cell types. Their phagocytic properties resemble those of endoneurial fibroblasts in peripheral nerve and they share similar cytological features with the cells in the vitreous body that produce hyaluronic acid (Ovalle and Dow, 1983). The vast array of secretory organelles seen in cells of the inner capsule (see Fig. 20) is consistent with a role in the synthesis and secretion of the glycosaminoglycan-rich periaxial matrix. Moreover, synthesis of the collagen and elastin that occupy the paracellular regions (Cooper and Gladden, 1974) may also constitute a primary function of cells of the inner capsule.

Fusimotor Endings

The form and distribution of motor nerve endings on mammalian intrafusal muscle fibers has been the subject of controversy (Boyd, 1981; Boyd and Smith, 1984; Barker and Banks, 1986). Not surprisingly, this aspect of muscle spindle research has received considerable attention by investigators who have attempted to clarify this issue from both structural and functional viewpoints. The evaluation of fusimotor nerve endings in this report does not attempt to resolve the issue, but rather, provides an example of how HRSEM can be utilized to clarify the three-dimensional morphology of fusimotor endings and their relationship to the underlying intrafusal fibers.

By HRSEM, fusimotor endings exhibited rounded neuronal profiles that often lay superficially, but in close apposition, to the underlying intrafusal fiber. Unlike sensory nerve terminals, they were covered externally by Schwann cell processes. When cleaved open, the terminal axoplasm was seen to contain numerous cellular organelles, the most prominent of which were mitochondria and synaptic vesicles. The mitochondria within motor endings, in

contrast to those in sensory endings, appeared pleomorphic in shape and were oriented in different directions. Their abundance in the fusimotor terminal is likely a reflection of high metabolic demand.

The postjunctional sarcoplasm of the intrafusal fiber was also typified by numerous mitochondria along with dilated cisternae of the SR. Extreme dilatations of the SR have been reported previously in intrafusal muscle fibers of other species (Smith and Ovalle, 1972). It has been postulated that these terminal dilatations of the SR provide for an increase in the rate of Ca^{2+} release and uptake, thus enhancing the rate of contraction and relaxation of the intrafusal fibers (Ovalle, 1971). In this context, the intimate association of the SR cisternae with the sarcolemma, and its proximity to the neuromuscular junction, is intriguing (see Fig. 21). It is tempting to speculate that, during neuromuscular transmission, such an arrangement enables the wave of depolarization to spread along the sarcolemma directly to the SR, thus bypassing the T-tubular system. This would enhance the speed of excitation-contraction coupling events and, in turn, influence the rate of muscle contraction. The close association of mitochondria to the SR cisternae may also have functional implications, although at present they remain enigmatic.

Sensory Endings

The three-dimensional morphology of sensory nerve endings on intrafusal fibers has been studied by TEM reconstruction techniques (Scalzi and Price, 1971; Kennedy et al., 1975; Banks et al., 1982; Banks, 1986), freeze-fracture electron microscopy (Quick, 1984), and conventional SEM (Schröder et al., 1988, 1989). The present report documents sensory-ending ultrastructure, for the first time, by HRSEM.

Primary and secondary sensory endings are thought to differ very little in terms of their ultrastructural makeup (Boyd and Smith, 1984). In this report, no attempt has been made to classify observations into either category but, rather, sensory-ending ultrastructure

has been described in general terms. All sensory terminals examined abounded with mitochondria. The shapes and sizes of these organelles, when viewed by conventional TEM, can be misleading. When sensory terminals are sectioned transversely, their mitochondria usually appear small and rounded (see Fig. 24). The present report has shown, in fact, that they can vary considerably both in shape and in size, and that the majority of mitochondria are elongated. Moreover, their arrangement and distribution is far easier to appreciate when individual terminals are viewed three-dimensionally. The observations are consistent with the notion that the majority of mitochondria are oriented in-parallel with the longitudinal axis of the sensory terminal (see Fig. 26). While the significance of this directionality is not known, there is evidence that mitochondria move up and down afferent axons in a bidirectional fashion (Smith, 1974). Orientation of the mitochondria in this manner would, thus, very likely facilitate such a process.

It is not entirely clear why mitochondria are so abundant in these regions. Their prominence, however, suggests that sensory terminals are sites of high metabolic demand. Regulation of Na⁺-channel activity (Hunt et al., 1978; Hunt, 1990) could account for some of these metabolic needs. In addition, the trophic influence that the sensory nerve supply is known to exert on the intrafusal fibers (Zelená and Soukup, 1973) may also require high levels of energy to maintain.

The membrane-bounded tubular profiles seen adjacent to the plasma membrane of the sensory nerve terminal are also noteworthy (see Fig. 25). The presence of similar structures as seen by TEM has been reported previously (Kennedy et al., 1975), and they have been interpreted as profiles of smooth-surfaced endoplasmic reticulum which are thought to play a role in the transport and turnover of intracellular materials. Another plausible role for these tubular structures might be the storage of cations, such as Ca²⁺, needed for sensory transduction events. Hunt and co-workers (1978) have in fact shown that when Na⁺ is absent in sensory nerve terminals, Ca²⁺ can partially substitute in producing receptor potentials.

Junctional couplings between the plasma membrane of sensory nerve terminals and the sarcolemma of intrafusal fibers have been observed in previous TEM studies (Düring and Andres, 1969; Mayr, 1970; Smith and Ovalle, 1972; Kennedy et al., 1975; Quick, 1984; Hikida, 1985). By conventional TEM, they appear as electron-dense regions that are disk-like in shape, and resemble the *fasciae adherentes* of cardiac muscle (Kennedy et al., 1975). By HRSEM, they appear as punctate bands that link the closely apposed membranes at irregularly spaced intervals in a zipper-like fashion (see Fig. 25). The functional significance of these membrane specializations is a matter of speculation. Kennedy and co-workers (1975) contend that these inter-membranous linkages transmit longitudinally-applied shear forces, created during muscle stretch, directly to the nerve cell membrane. Presumably, the resultant distortion of the membrane produces an increase in Na⁺ conductance which, according to Hunt and co-workers (1978), leads to generation of receptor potentials. The frequency by which these membrane specializations were visualized by HRSEM would certainly emphasize their physiological importance. On the other hand, they may simply serve to mechanically anchor sensory endings, thus maintaining their spatial orientation and positioning relative to the underlying intrafusal fibers.

An alternative hypothesis concerning the mechanics of sensory transduction in the muscle spindle has been put forth by Banks and co-workers (1982). They suggest that sensory transduction is a result of nerve-terminal compression, and that sensory endings are deformed in their entirety rather than at individual sites. According to them, the source of this compression comes from longitudinally-arranged elements such as intrafusal fibers and their associated external laminae, which together transmit tension in response to muscle stretch. In the present SEM study, the intricate encasement of external laminae that was seen three-dimensionally around intrafusal fibers and their sensory endings lends credence to this hypothesis (see Figs. 19 and 26). Moreover, the presence of elastic tissue in these regions is consistent with the view that they are designed to accommodate stretch (Cooper and Gladden,

1974).

The pleated appearance of the nerve cell membrane at the sensory terminal (see Figs. 24, 26) may also be of physiological significance in terms of sensory transduction. According to Banks (1986), corrugations in the neuronal membrane are likely maintained by membrane-associated cytoskeletal filaments. Presumably, these corrugations allow the membrane to accommodate changes in surface area that result from terminal compression. Sensory transduction is then thought to be achieved via the transmission of increased tension to the cytoskeletal filaments in response to changes in membrane surface area. The present observations made by HRSEM provide structural evidence for such a mechanism as they also demonstrate a network of axoplasmic filaments within sensory terminals (see Fig. 26). Moreover, the filaments appear to be anchored to the neuronal membrane in regular fashion, giving the membrane its pleated appearance.

Kennedy and co-workers (1974) have reported the presence of a microfilament network in the periphery of sensory nerve terminals in human muscle spindles. By TEM, they described these filaments as "actin-like", postulating that they may enable the endings to adapt to force changes brought about by muscle stretch. The possibility also exists that these filaments are involved in the mechanics of axoplasmic transport, particularly in the bidirectional movement of mitochondria along the sensory axon and in the nerve terminal (Smith, 1974).

In summary, a complete appreciation of the fine structure of muscle spindles can be achieved only through analysis with a variety of methodologies. Conventional and high resolution SEM have been used in this report to visualize spindle morphology from a three-dimensional perspective. It is hoped that a more complete understanding of the intricate ultrastructural makeup of these unique neuromuscular receptors will contribute towards a better understanding of their complex functions.

CONCLUSIONS AND FUTURE DIRECTIONS

This study was undertaken to provide a better understanding of the complex three-dimensional ultrastructure of muscle spindles. It also served to evaluate the hamster tenuissimus muscle in terms of its suitability as a model for the study of muscle spindles, in particular for scanning electron microscopy.

This study demonstrated that the hamster tenuissimus is one of the most heavily populated of all skeletal muscles yet studied in terms of muscle spindle content. This fact, coupled with its rather sparse population of extrafusal fibers, suggests that the muscle may play a critical role in hindlimb sensory feedback. It is worthwhile noting that the animals which possess this muscle (hamsters, mink, rabbits, cats) all have the ability to sit or stand on their hindlimbs while using their forelimbs for independent activity. Could the tenuissimus muscle represent an adaptive mechanism aimed at providing these animals with greater hindlimb proprioceptive capabilities in these situations? To answer such a question would require an in-depth physiological and morphological evaluation of the muscle *in situ*. It would be interesting to determine, however, if other animals, such as the squirrel and the racoon, also possess this muscle. Both of these animals have similar postural capabilities.

The high spindle density/low extrafusal fiber arrangement also makes the hamster tenuissimus ideal for the microdissection of individual muscle spindles for further morphological and/or physiological evaluation. In the present study isolated spindle preparations were examined by fluorescence and scanning electron microscopy. The muscle is also ideal for use in the HRSEM evaluation of these receptors. The high spindle density makes it very likely that a spindle profile will be obtained regardless of where the muscle is freeze-cleaved. This has important considerations in terms of the working time required to process a specimen completely for microscopic evaluation.

Virtually all aspects of spindle morphology could be clearly observed by HRSEM in this study. Because of the tremendous amount of information captured in each micrograph, however, interpretations are sometimes not easy. Comparisons with other methodologies, particularly TEM, are valuable in this regard.

Continued work along these lines will no doubt provide additional findings of interest. The further application of fluorescence microscopy and of immunocytochemical techniques to isolated spindle preparations holds great promise. For example, the distribution of proteins, such as the isoforms of myosin, along with certain membrane-associated proteins, such as dystrophin, could be readily visualized along the axial length of intrafusal fibers. Comparisons of these distributions amongst the various fiber types could then be made with considerable ease. Alterations in their distribution could also be elucidated in certain pathological processes.

HRSEM is another technique that holds great potential for further spindle research. A detailed evaluation of the intrafusal fibers of spindles is an area that clearly needs to be explored in greater detail. Further assessment of the complex fusimotor innervation of the spindle using this technique might provide further clues regarding its relationship with the central nervous system. Combining state-of-the-art immunocytochemical techniques with HRSEM will enhance even further its usefulness in muscle spindle research and in skeletal muscle research in general.

A more complete understanding of muscle spindle ultrastructure will contribute greatly towards a better understanding of their function. Furthermore, it will facilitate the assessment of pathological effects, if any, brought on by certain disease processes or by physical trauma. It is hoped that the present findings will provide a morphological and three-dimensional basis for the further evaluation of these complex neuromuscular receptors.

LITERATURE CITED

- Adal, M.N. 1969 The fine structure of the sensory region of cat muscle spindles. *J. Ultrastruct. Res.*, 26: 332-354.
- Adrian, E.D. 1925 The spread of activity in the tenuissimus muscle of the cat and in other complex muscles. *J. Physiol. (Lond.)*, 60: 301-315.
- Arbuthnott, E.R., K.J. Ballard, I.A. Boyd, M.H. Gladden, and F.I. Sutherland 1982 The ultrastructure of the cat fusimotor endings and their relationship to foci of sarcomere convergence in intrafusal fibers. *J. Physiol. (Lond.)*, 331: 285-309.
- Bakker, G.J., and F.J.R. Richmond 1981 Two types of muscle spindles in cat neck muscles: A histochemical study of intrafusal fiber composition. *J. Neurophysiol.*, 45: 973-986.
- Bakker, G.J., and F.J. R. Richmond 1982 Muscle spindle complexes in muscles around upper cervical vertebrae in the cat. *J. Neurophysiol.*, 48: 62-74.
- Banker, B.Q., and J.P. Girvin 1971 The ultrastructural features of the mammalian muscle spindle. *J. Neuropath. Exp. Neurol.*, 30: 155-195.
- Banks, R.W. 1981a The number and distribution of satellite cells of intrafusal muscle fibers in a muscle spindle of the cat. *J. Anat.*, 133: 694.
- Banks, R.W. 1981b A histological study of the motor innervation of the cat's muscle spindle. *J. Anat.*, 133: 571-591.
- Banks, R.W. 1986 Observations on the primary sensory ending of tenuissimus muscle spindles in the cat. *Cell Tissue Res.*, 246: 309-319.
- Banks, R.W., D. Barker, P Bessou, B Pages, and M.J. Stacey 1978 Histological analysis of cat muscle spindles following direct observation of the effects of stimulating dynamic and static motor axons. *J. Physiol. (Lond.)*, 283: 605-619.
- Banks, R.W., D. Barker, and M.J. Stacey 1982 Form and distribution of sensory terminals in cat hindlimb muscle spindles. *Philos. Trans. R. Soc. Lond. (Biol.)*, 299: 329-364.
- Banks, R.W., D. Barker, and M.J. Stacey 1985 Form and classification of motor endings in mammalian muscle spindles. *Proc. R. Soc. Lond. (Biol.)*, 225: 195-212.
- Banks, R.W., D.W. Harker, and M.J. Stacey 1977 A study of mammalian intrafusal muscle fibers using a combined histochemical and ultrastructural technique. *J. Anat.*, 123: 783-796.
- Barker, D. 1974 The morphology of muscle receptors. In: *Muscle Receptors. Handbook of Sensory Physiology*. C.C. Hunt, ed. Springer-Verlag, Berlin, Vol 1, Pt 2, pp. 1-190.
- Barker, D., and R.W. Banks 1986 The muscle spindle. In: *Myology*. A.G. Engel and B.Q. Banker, eds. McGraw-Hill, New York, Vol 1, pp. 309-341.
- Barker, D., and N.K. Chin 1960 The number and distribution of muscle spindles in certain muscles of the cat. *J. Anat.*, 94: 473-486.

- Barker, D., F. Emonet-Dénand, D.W. Harker, L. Jami, and Y. Laporte 1976 Distribution of fusimotor axons to intrafusal muscle fibers in cat tenuissimus spindles as determined by the glycogen-depletion method. *J. Physiol. (Lond.)*, 261: 49-69.
- Barker, D., F. Emonet-Dénand, D.W. Harker, L. Jami, and Y. Laporte 1977 Types of intra- and extrafusal muscle fibers innervated by dynamic skeletofusimotor axons in cat peroneus brevis and tenuissimus muscles, as determined by the glycogen-depletion method. *J. Physiol. (Lond.)*, 266: 713-726.
- Barker, D., F. Emonet-Dénand, Y. Laporte, and M.J. Stacey 1980 Identification of the intrafusal endings of skeletofusimotor axons in the cat. *Brain Res.*, 185: 227-237.
- Barker, D., M.J. Stacey, and M.N. Adal 1970 Fusimotor innervation in the cat. *Philos. Trans. R. Soc. Lond. (Biol.)*, 258: 315-346.
- Bensley, B.A. 1921 *Practical Anatomy of the Rabbit*. University of Toronto, pp., 217-234.
- Boyd, I.A. 1956 The tenuissimus muscle of the cat. *J. Physiol. (Lond.)*, 133: 35-36P.
- Boyd, I.A. 1981 The muscle spindle controversy. *Sci. Prog. Oxf.*, 67: 205-221.
- Boyd, I.A., and R.S. Smith 1984 The muscle spindle. In: *Peripheral Neuropathy*. P.J. Dyck, P.K. Thomas, E.H. Lambert, and R. Bunge, eds. W.B. Saunders, Philadelphia, Vol 1, pp. 171-202.
- Bridgman, C.F., and E. Eldred 1964 Hypothesis for a pressure-sensitive mechanism in muscle spindles. *Science*, 143: 481-482.
- Brzezinski, D.K. von 1961a Untersuchungen zur Histochemie der Muskelspindeln. I. Mitteilung: Topochemie der Polysaccharide. *Acta Histochem.*, 12: 75-79.
- Brzezinski, D.K. von 1961b Untersuchungen zur Histochemie der Muskelspindeln. II. Mitteilung: Zur Topochemie und Funktion des Spindelraumes und der Spindelkapsel. *Acta Histochem.*, 12: 277-288.
- Butler, R. 1979 A new grouping of intrafusal muscle fibers based on developmental studies of muscle spindles in the cat. *Am. J. Anat.*, 156: 115-120.
- Butler, R. 1980 The organization of muscle spindles in the tenuissimus muscle of the cat during late development. *Develop. Biol.*, 77: 191-212.
- Cooper, S. 1960 Muscle spindles and other muscle receptors. In: *The Structure and Function of Muscle*. G.H. Bourne, ed. Academic Press, New York, pp. 381-420.
- Cooper, S., and M.H. Gladden 1974 Elastic fibres and reticulin of mammalian muscle spindles and their functional significance. *Q. J. Exp. Physiol.*, 59: 367-385.
- Corjava, N., V. Marinozzi, and O. Pompeiano 1969 Muscle spindles in the lumbrical muscle of the adult cat. *Arch. Ital. Biol.*, 107: 365-543.
- Desaki, J., and Y. Uehara 1981 The overall morphology of neuromuscular junctions as revealed by scanning electron microscopy. *J. Neurocytol.*, 10: 101-110.

- Desaki, J., and Y. Uehara 1983 A fine structural study of the termination of intrafusal muscle fibres in the Chinese hamster. *Cell Tissue Res.*, 234: 723-733.
- Dow, P.R., S.L. Shinn, and W.K. Ovalle 1980 Ultrastructural study of a blood-muscle spindle barrier after systemic administration of horseradish peroxidase. *Am. J. Anat.*, 157: 375-388.
- Dubowitz, V., and M.H. Brooke 1973 *Muscle Biopsy: A Modern Approach*. W. B. Saunders, Philadelphia, pp. 5-73.
- Düring, M., and K.H. Andres 1969 Zur Feinstruktur der Muskelspindel von Mammalia. *Anat. Anz.*, 124: 566-573.
- Eccles, J.C., and C.S. Sherrington 1930 Numbers and contraction-values of individual motor-units examined in some muscles of the limb. *Proc. R. Soc. Lond. (Biol.)*, 106: 326-357.
- Edwards, R. 1975 An ultrastructural study of neuromuscular spindles in normal mice: With reference to mice and man infected with *Myobacterium leprae*. *J. Anat.*, 20: 149-168.
- Eriksson, E., and B. Lisander 1972 Low flow states in the microvessels of skeletal muscle in the cat. *Acta Physiol. Scand.*, 86: 202-210.
- Eriksson, E., and R. Myrhage 1972 Microvascular dimensions and blood flow in skeletal muscle. *Acta Physiol. Scand.*, 86: 211-222.
- Evan, A.P., W.G. Dail, D. Dammrose, and C. Palmer 1976 Scanning electron microscopy of cell surfaces following removal of extracellular material. *Anat. Rec.*, 185: 433-446.
- Farrell, P.R., and M.R. Fedde 1969 Uniformity of structural characteristics throughout the length of skeletal muscle fibers. *Anat. Rec.*, 164: 219-220.
- Fukami, Y. 1982 Further morphological and electrophysiological studies on snake muscle spindles. *J. Neurophysiol.*, 47: 810-826.
- Fukami, Y. 1986 Studies of capsule and capsular space of cat muscle spindles. *J. Physiol. (Lond.)*, 376: 281-297.
- Fukami, Y., and P.H. Schlesinger 1989 Endocytosis and transcytosis by the capsule cell of vertebrate muscle spindles. *Brain Res.*, 499: 249-257.
- Griep, E.B., and E.S. Robbins 1988 Epithelium. In: *Cell and Tissue Biology. A Textbook of Histology*. L. Weiss, ed. Urban and Schwarzenberg, Baltimore, pp.113-153.
- Harker, D.W., L. Jami, Y. Laporte, and J. Petit 1977 Fast conducting skeletofusimotor axons supplying intrafusal chain fibers in the cat peroneus-tertius muscle. *J. Neurophysiol.*, 40: 791-799.
- Hikida, R.S. 1985 Spaced serial section analysis of the avian muscle spindle. *Anat. Rec.*, 212: 255-267.
- Hollenberg, M.J., and A.M. Erickson 1973 The scanning electron microscope: potential usefulness to biologists. *J. Histochem. Cytochem.*, 21: 109-130.

- Hollenberg, M.J., D.H. Cormack, and P.J. Lea 1989 Stereo Atlas of the Cell. B.C. Decker, Toronto, pp. 1-129.
- Hollenberg, M.J., and P.J. Lea 1988 High resolution scanning electron microscopy of the retinal pigment epithelium and Bruch's layer. *Invest. Ophthalmol. Vis. Sci.*, 29: 1380-1389.
- Hunt, C.C. 1990 Mammalian muscle spindle: peripheral mechanisms. *Phys. Rev.*, 70: 643-663.
- Hunt, C.C., and S.W. Kuffler 1951 Further study of efferent small-nerve fibres to mammalian muscle spindles. Multiple spindle innervation and activity during contraction. *J. Physiol. (Lond.)*, 113: 283-297.
- Hunt, C.C., R.S. Wilkinson, and Y. Fukami 1978 Ionic basis of the receptor potential in primary endings of mammalian muscle spindles. *J. Gen. Physiol.*, 71: 683-698.
- James, N.T. 1971 The histochemical demonstration of mucopolysaccharide in the lymph space of muscle spindles. *J. Anat.*, 110: 163.
- James, N.T., and G.A. Meek 1973 An electron microscopic study of avian muscle spindles. *J. Ultrastruct. Res.*, 43: 193-204.
- Johnson, M.J., and W.K. Ovalle 1986 A comparative study of muscle spindles in slow and fast neonatal muscles of normal and dystrophic mice. *Am. J. Anat.*, 175: 413-427.
- Karlsson, U., E. Andersson-Cedergren, and D. Ottoson 1966 Cellular organization of the frog muscle spindle as revealed by serial sections for electron microscopy. *J. Ultrastruct. Res.*, 14: 1-35.
- Katz, B. 1961 The terminations of the afferent nerve fibre in the muscle spindle of the frog. *Philos. Trans. R. Soc. Lond. (Biol.)*, 243: 221-240.
- Kennedy, W.R., R.E. Poppele, and D.C. Quick 1980 Mammalian muscle spindles. In: *The Physiology of Peripheral Nerve Disease*. A.J. Sumner, ed. W.B. Saunders, Philadelphia, pp. 75-132.
- Kennedy, W.R., H. deF. Webster, and K.S. Yoon 1975 Human muscle spindles: fine structure of the primary sensory ending. *J. Neurocytol.*, 4: 675-695.
- Kennedy, W.R., H. deF. Webster, K.S. Yoon, and D.H. Jean 1974 Human muscle spindles: microfilaments in the group 1A sensory nerve endings. *Anat. Rec.*, 180: 521-532.
- Kennedy, W.R., and K.S. Yoon 1979 Permeability of muscle spindle capillaries and capsule. *Muscle Nerve*, 2: 101-108.
- Khan, M.A., and T. Soukup 1979 Histo enzymatic study of rat intrafusal muscle fibers. *Histochemistry*, 62: 179-189.
- te Kronnie, G., Y. Donselaar, T. Soukup, and W. van Raamsdonk 1981 Immunohistochemical differences in myosin composition among intrafusal muscle fibers. *Histochemistry*, 73: 65-74.
- Kucera, J. 1980a Histochemical study of long nuclear chain fibers in the cat muscle spindle. *Anat. Rec.*, 198: 567-580.

- Kucera, J. 1980b Myofibrillar ATPase activity of intrafusal fibers in chronically deafferented rat muscle spindles. *Histochem.*, 66: 221-228.
- Kucera, J. 1981 Histochemical profiles of cat intrafusal muscle fibers and their motor innervation. *Histochemistry*, 73: 397-418.
- Kucera, J. 1982a Morphometric studies on tenuissimus muscle spindles in the cat. *J. Morphol.*, 171: 137-150
- Kucera, J. 1982b One-bag-fiber muscle spindles in tenuissimus muscles of the cat. *Histochemistry*, 76: 315-328.
- Kucera, J. 1982c Histological study of an unusual cat muscle spindle deficient in motor innervation. *Anat. Embryol.*, 165: 39-49.
- Kucera, J. 1983 Multiple-bag-fiber muscle spindles in tenuissimus muscles of the cat. *Histochemistry*, 79: 457-476.
- Kucera, J., and K. Dorovini-Zis 1979 Types of human intrafusal muscle fibers. *Muscle Nerve*, 2: 437-451.
- Kucera, J., and J.M. Walro 1989 Nonuniform expression of myosin heavy chain isoforms along the length of cat intrafusal muscle fibers. *Histochemistry*, 92: 291-299.
- Kühne, W. 1864 Über die Endigung der Nerven in den Nervenbügeln der Muskeln. *Virchows Arch. Path. Anat.*, 30: 187-220.
- Landon, D.N. 1966 Electron microscopy of muscle spindles. In: *Control and Innervation of Skeletal Muscle*. B.L. Andrew, ed. Livingstone, Edinburgh, pp. 96-111.
- Lea, P.J., and M.J. Hollenberg 1988 Mitochondrial structure revealed by high-resolution scanning electron microscopy. *Am. J. Anat.*, 184: 245-257.
- Lea, P.J., and S.A. Ramjohn 1980 Investigating the substitution of ethanol with liquid carbon dioxide during critical point drying. *Microsc. Acta*, 83: 291-296.
- Leksell, L. 1945 The action potential and excitatory effects of the small ventral root fibers to skeletal muscle. *Acta Physiol. Scand. (Suppl.)*, 10: 1-84.
- Lev-Tov, A., C.A. Pratt, and R.E. Burke 1988 The motor-unit population of the cat tenuissimus muscle. *J. Neurophysiol.*, 59: 1128-1142.
- Loeb, G.E., C.A. Pratt, C.M. Chanaud, and F.J.R. Richmond 1987 Distribution and innervation of short, interdigitated muscle fibers in parallel-fibered muscles of the cat hindlimb. *J. Morphol.*, 191: 1-15.
- Low, F.N. 1976 The perineurium and connective tissue of peripheral nerve. In: *The Peripheral Nerve*. D.N. Landon, ed. Chapman and Hall, London, pp. 159-187.
- Maier, A., B. Gambke, and D. Pette 1988 Immunohistochemical demonstration of embryonic myosin heavy chains in adult mammalian intrafusal fibers. *Histochemistry*, 88: 267-271.

- Maier, A., and R. Mayne 1987 Distribution of connective tissue proteins in chick muscle spindles as revealed by monoclonal antibodies: a unique distribution of brachionectin/tenascin. *Am. J. Anat.*, *180*: 226-236.
- Mayr, R. 1970 Zwei elektronenmikroskopisch unterscheidbare Formen sekundärer sensorischer Endigungen in einer Muskelspindel der Ratte. *Z. Zellforsch.* *110*: 97-107.
- Merrillees, N.C.R. 1960 The fine structure of muscle spindles in the lumbrical muscles of the rat. *J. Biophys. Biochem. Cytol.*, *7*: 725-742.
- Milburn, A. 1973 The early development of muscle spindles in the rat. *J. Cell Sci.*, *12*: 175-195.
- Miller, M.E. 1964 *Anatomy of the Dog*. W.B. Saunders, Philadelphia, pp. 231-247.
- Miyoshi, T., and W.R. Kennedy 1979a Microvasculature of rabbit muscle spindles. *Arch. Neurol.*, *36*: 471-475.
- Nemeth, P.M., D. Pette, and G. Vrbova 1981 Comparison of enzyme activities among single muscle fibers within defined motor units. *J. Physiol. (Lond.)*, *311*: 489-495.
- Novikoff, A.B., W. Shin, and J. Drucker 1961 Mitochondrial localization of oxidative enzymes: staining results with two-tetrazolium salts. *J. Biophys. Biochem. Cytol.*, *9*: 47-61.
- Ovalle, W.K. 1971 Fine structure of rat intrafusal muscle fibers. The polar region. *J. Cell Biol.*, *51*: 83-103.
- Ovalle, W.K. 1972a Fine structure of rat intrafusal muscle fibers. The equatorial region. *J. Cell Biol.*, *52*: 382-396.
- Ovalle, W.K. 1972b Motor nerve terminals on rat intrafusal muscle fibres, a correlated light and electron microscopic study. *J. Anat.*, *111*: 239-252.
- Ovalle, W.K. 1976 Fine structure of the avian muscle spindle capsule. *Cell Tissue Res.*, *166*: 285-298.
- Ovalle, W.K., and P.R. Dow 1983 Comparative ultrastructure of the inner capsule of the muscle spindle and the tendon organ. *Am. J. Anat.*, *166*: 343-357.
- Ovalle, W.K., and P.R. Dow 1986 Alterations in muscle spindle morphology in advanced stages of murine muscular dystrophy. *Anat. Rec.*, *216*: 111-126.
- Ovalle, W.K., and P.R. Dow 1988 The capsular sleeve of muscle spindles in mouse and man with special reference to the cytoskeleton. In: *Mechanoreceptors. Development, Structure and Function*. P. Hník, T. Soukup, R. Vejsada, and J. Zelená, eds. Plenum, New York, pp. 255-261.
- Ovalle, W.K., and R.S. Smith 1972 Histochemical identification of three types of intrafusal muscle fibers in the cat and monkey based on the myosin ATPase reaction. *Can. J. Physiol. Pharm.*, *50*: 195-202.
- Patten, R.M., and W.K. Ovalle 1990 Three dimensional morphology of intact muscle spindles isolated from the hamster tenuissimus. *Anat. Rec.*, *226*: 78A.

- Patten, R.M., and W.K. Ovalle 1991 Muscle spindle ultrastructure revealed by conventional and high resolution scanning electron microscopy. *Anat. Rec.*, (in press).
- Peck, D., D.F. Buxton, and A. Nitz 1984 A comparison of spindle concentrations in large and small muscles acting in parallel combinations. *J. Morphol.*, 180: 243-252.
- Pette, D., M. Wimmer, and P. Nemeth 1980 Do enzyme activities vary along muscle fibers? *Histochemistry*, 67: 225-231.
- Pierobon-Bormioli, S., S. Sartore, M. Vitadello, and S. Schiaffino 1980 "Slow" myosins in vertebrate skeletal muscle. An immunofluorescence study. *J. Cell Biol.*, 85: 672-681.
- Porter, K.R., and F. Kallman 1953 The properties and effects of osmium tetroxide as a tissue fixative with special reference to its use for electron microscopy. *Exp. Cell Res.*, 4: 127-141.
- Quick, D.C. 1984 Freeze-fracture of sensory nerve endings in cat muscle spindles. *J. Neurocytol.*, 13: 975-987.
- Reiss, K.R., and D.M. Noden 1989 SEM characterization of a cellular layer separating blood vessels from endoderm in the quail embryo. *Anat. Rec.*, 225: 165-175.
- Reynolds, E.S. 1963 The use of lead citrate at high pH as an electron-opaque stain for electron microscopy. *J. Cell Biol.*, 17: 208.
- Rogers, S.L., and B.M. Carlson 1981 A quantitative assessment of muscle spindle formation in reinnervated and non-reinnervated grafts of the rat extensor digitorum longus muscle. *Neuroscience*, 6: 87-94.
- Rowlerson, A., L. Gorza, and S. Schiaffino 1985 Immunohistochemical identification of spindle fiber types in mammalian muscle using type-specific antibodies to isoforms of myosin. In: *The Muscle Spindle*. I.A. Boyd and M.H. Gladden, eds. Macmillan, London, pp. 29-34.
- Ruffini, A. 1898 On the minute anatomy of the neuromuscular spindles of the cat, and on their physiological significance. *J. Physiol. (Lond.)*, 23: 190-208.
- Scalzi, H.A., and H.M. Price 1971 The arrangement and sensory innervation of the intrafusal fibers in the feline muscle spindle. *J. Ultrastruct. Res.*, 36: 375-390.
- Schröder, J.M. 1974 The fine structure of de- and reinnervated muscle spindles. 1. The increase, atrophy, and "hypertrophy" of intrafusal muscle fibers. *Acta Neuropathol. (Berl.)*, 30: 109-128.
- Schröder, J.M., H. Bodden, A. Hamacher, and C. Verres 1988 Scanning electron microscopic identification of motor and sensory endings on teased intrafusal muscle fibers. In: *Mechanoreceptors. Development, Structure and Function*. P. Hník, T. Soukup, R. Vejsada, and J. Zelená, eds. Plenum, New York, pp. 237-240.
- Schröder, J.M., H. Bodden, A. Hamacher, and C. Verres 1989 Scanning electron microscopy of teased intrafusal muscle fibers from rat muscle spindles. *Muscle Nerve*, 12: 221-232.
- Shantha, T.H., and G.H. Bourne 1968 The perineurial epithelium - a new concept. In: *The Structure and Function of the Nervous System*. G.H. Bourne, ed. Academic Press, New York, Vol 1, pp. 379-459.

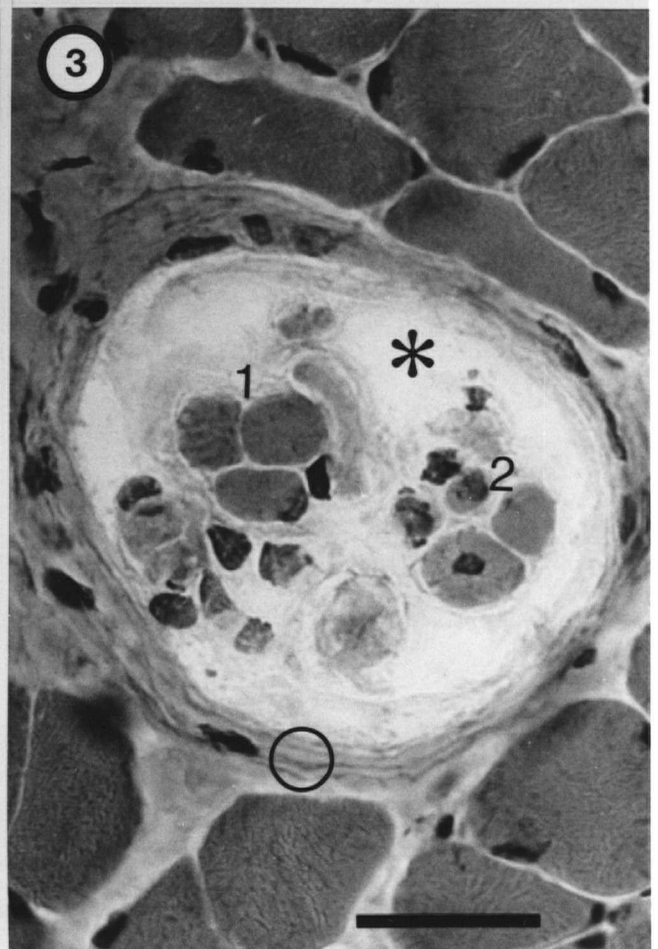
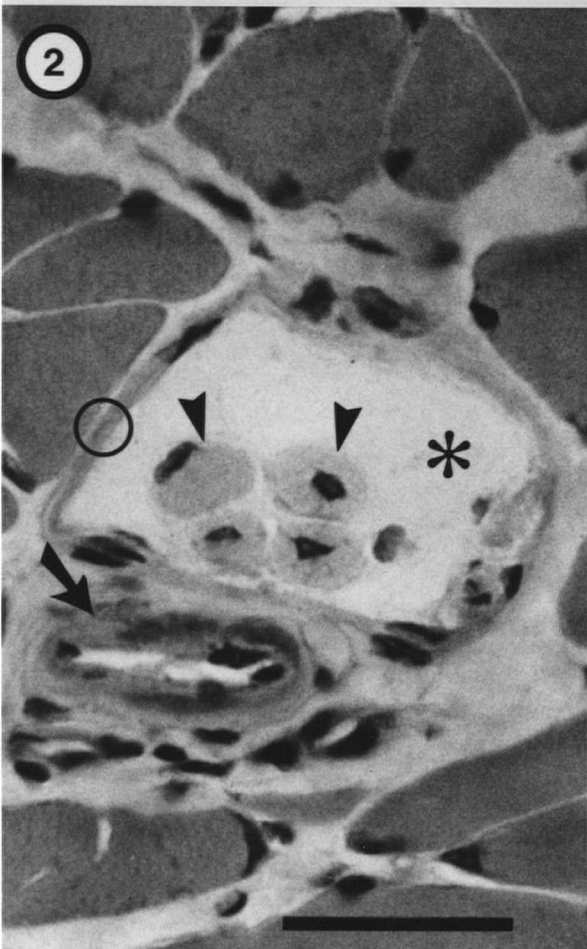
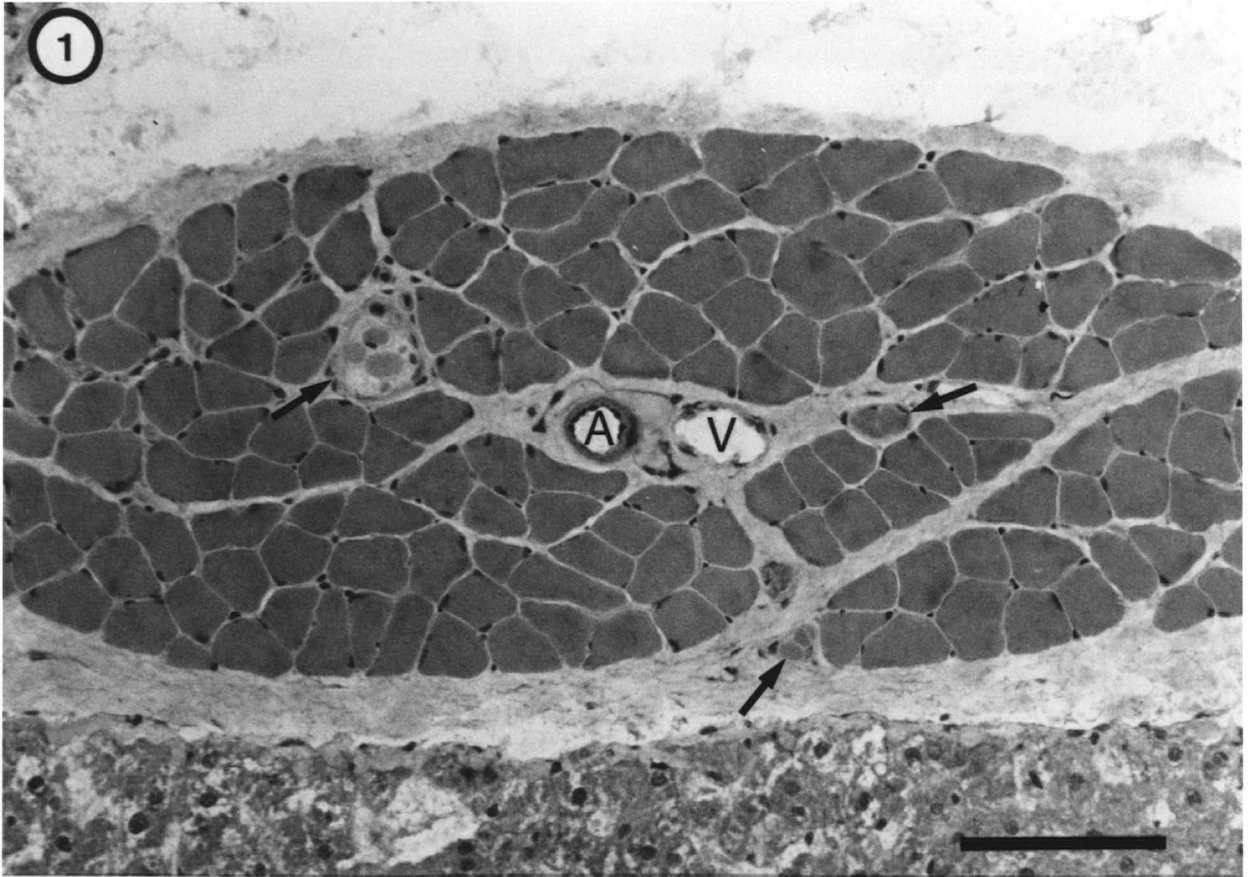
- Shantha, T.H., M.N. Golarz, and G.H. Bourne 1968 Histological and histochemical observations on the capsule of the muscle spindle in normal and denervated muscle. *Acta Anat.*, 69: 632-646.
- Sherrington, C.S. 1894 On the anatomical constitution of nerves to skeletal muscles; with remarks on recurrent fibers in the ventral spinal nerve-root. *J. Physiol. (Lond.)*, 17: 211-258.
- Simionescu, N., M. Simionescu, and G.E. Palade 1975 Permeability of muscle capillaries to small heme-peptides. Evidence for the existence of patent transendothelial channels. *J. Cell Biol.*, 64: 586-607.
- Sjöstrand, F.S. 1989 Common sense in electron microscopy. About osmium fixation. *J. Ultrastruct. Mol. Struct. Res.*, 102: 1-8.
- Smith, R.S. 1974 The movement of mitochondria at sensory endings in the muscle spindle. *J. Anat.*, 119: 194.
- Smith, R.S., and W.K. Ovalle 1972 The structure and function of intrafusal muscle fibers. In: *Muscle Biology*. R.G. Cassens, ed. Marcel Dekker, New York, Vol 1, pp. 147-227.
- Soukup, T. 1976 Intrafusal fiber types in rat limb muscle spindles. Morphological and histochemical characteristics. *Histochemistry*, 47: 43-57.
- Staron, R.S., and D. Pette 1986 Correlation between myofibrillar ATPase activity and myosin heavy chain composition in rabbit muscle fibers. *Histochemistry*, 86: 19-23.
- Swash, M., and K.P. Fox 1974 The pathology of the human muscle spindle: effect of denervation. *J. Neurol. Sci.*, 22: 1-24.
- Swett, J.E., and E. Eldred 1960 Distribution and number of stretch receptors in medial gastrocnemius and soleus muscles of the cat. *Anat. Rec.*, 137: 453-460.
- Tanaka, K. 1972 Freezed resin cracking method for scanning electron microscopy of biological materials. *Naturwissenschaften*, 59: 77.
- Tanaka, K., and A. Mitsushima 1984 A preparation method for observing intracellular structures by scanning electron microscopy. *J. Microsc.*, 133: 213-222.
- Vesely, P., and A. Boyde 1973 The significance of SEM evaluation of the cell surface for tumor cell biology. In: *Scanning Electron Microscopy*. O. Johari and I. Corvin, eds. IITRI, Chicago, pp. 689-696.
- Voss, H. 1937 Untersuchungen über Zahl, Anordnung und Länge der Muskelspindeln in den Lumbricalmuskeln des Menschen und einiger Tiere, *Z. Mikrock. Anat. Forsch.*, 42: 509-524.
- Walker, W.F. 1980 *Vertebrate Dissection*. Saunders College, Philadelphia, pp. 157-168.
- Weismann, A. 1861 Über das Waschen der auergestreiften Muskeln nach Beobachtungen am Frosch. *Z. Rat. Med.*, 10: 263-284.
- Yellin, H. 1969a A histochemical study of muscle spindles and their relationship to extrafusal fiber types in the rat. *Am. J. Anat.*, 125: 31-46.

- Yellin, H. 1969b Unique intrafusal and extraocular muscle fibers exhibiting dual actomyosin ATPase activity. *Exp. Neurol.*, 25: 153-163.
- Zelená, J., and T. Soukup 1973 Development of muscle spindles deprived of fusimotor innervation. *Z. Zellforsch. Mikrosk. Anat.*, 144: 435-452.
- Zelená, J., and T. Soukup 1974 The differentiation of intrafusal fiber types in rat muscle spindles after motor denervation. *Cell Tissue Res.*, 153: 115-136.

Fig. 1. Low magnification light micrograph of a tenuissimus muscle cut in cross-section and stained with H & E. Profiles of three muscle spindles (arrows) can be seen embedded within a matrix of perimysial connective tissue. The main muscle artery (A) and vein (V) are located centrally within a closely packed array of extrafusal fibers. x265. Bar = 100 μ m.

Fig. 2. Higher magnification light microscopic view of a muscle spindle in the juxtaequatorial region stained with H & E. Two bag (arrowheads) and two chain (not labelled) intrafusal fibers sit within a prominent periaxial space (asterisk). A small blood vessel (arrow) is closely associated with the outer spindle capsule (circle). x980. Bar = 30 μ m.

Fig. 3. Cross-sectional light microscopic view of a tandem muscle spindle in the juxtaequatorial region stained with H & E. Two separate sets of intrafusal fibers (numbered 1 and 2) share a common periaxial space (asterisk). A prominent outer capsule envelops the entire spindle complex (circle). x790. Bar = 30 μ m.



4

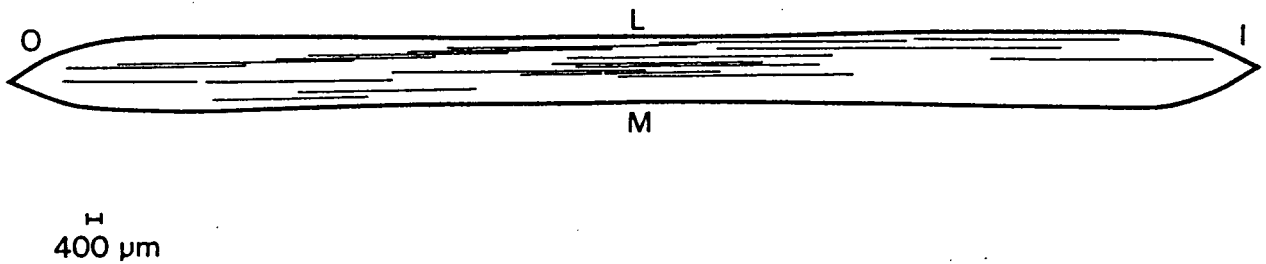


Fig. 4. Longitudinal reconstruction showing the distribution and lengths of muscle spindles in the tenuissimus muscle of the hamster. Each line designates one spindle. The origin (O), insertion (I), and medial (M) and lateral (L) borders are all indicated.

Table I. Summary of muscle spindle quantitative data.

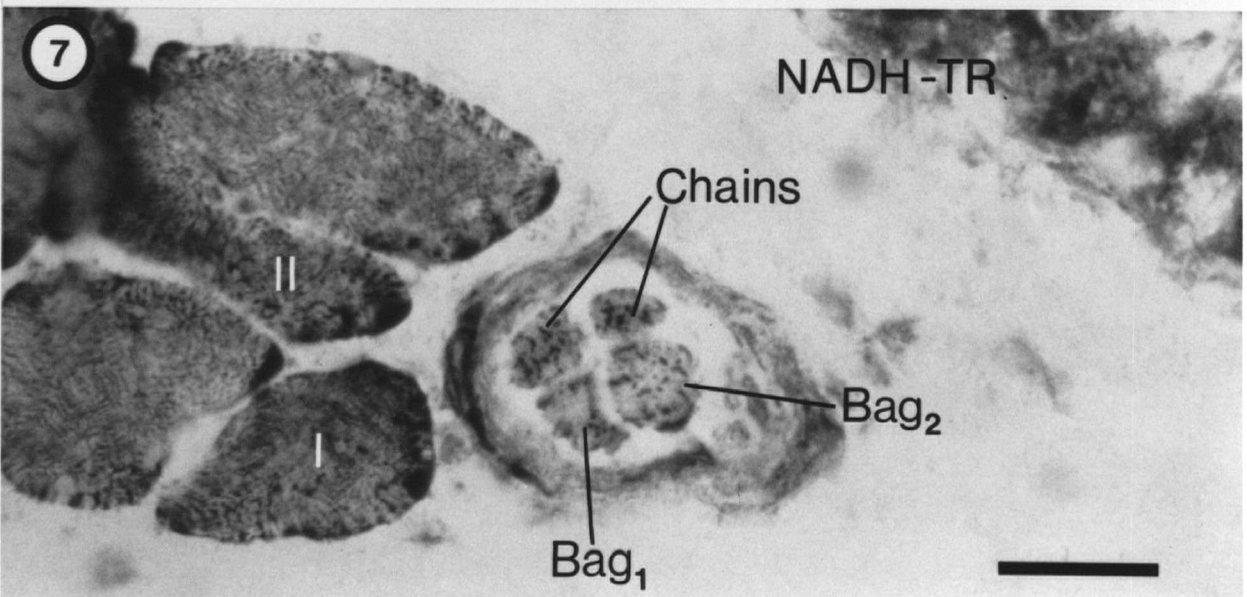
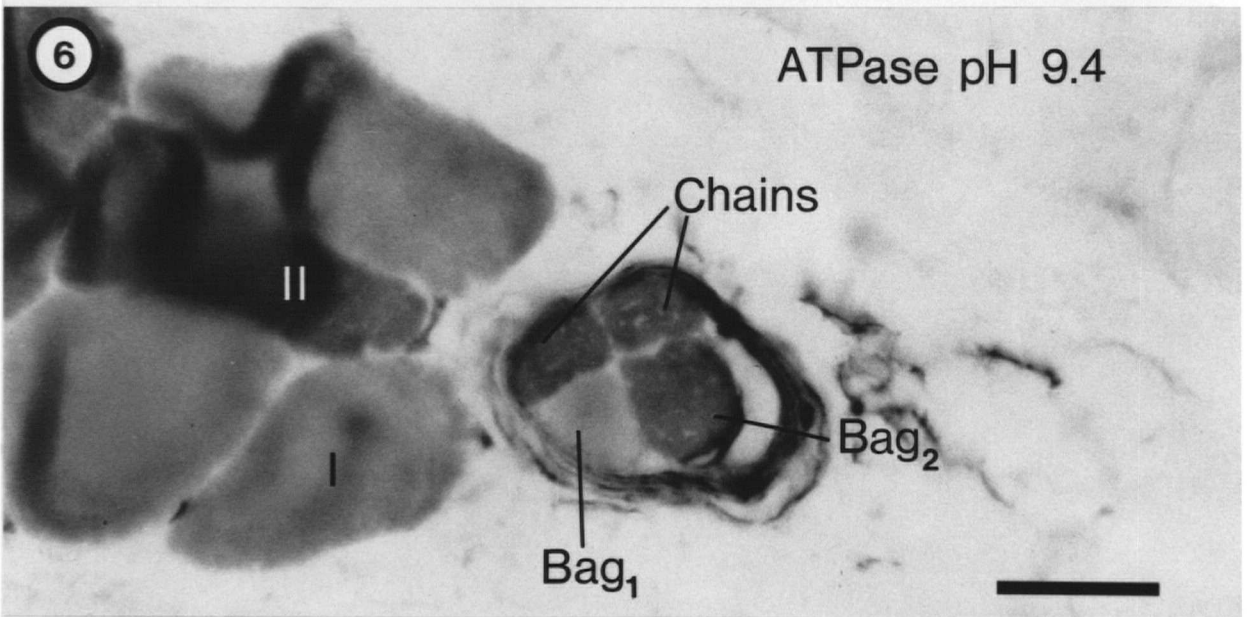
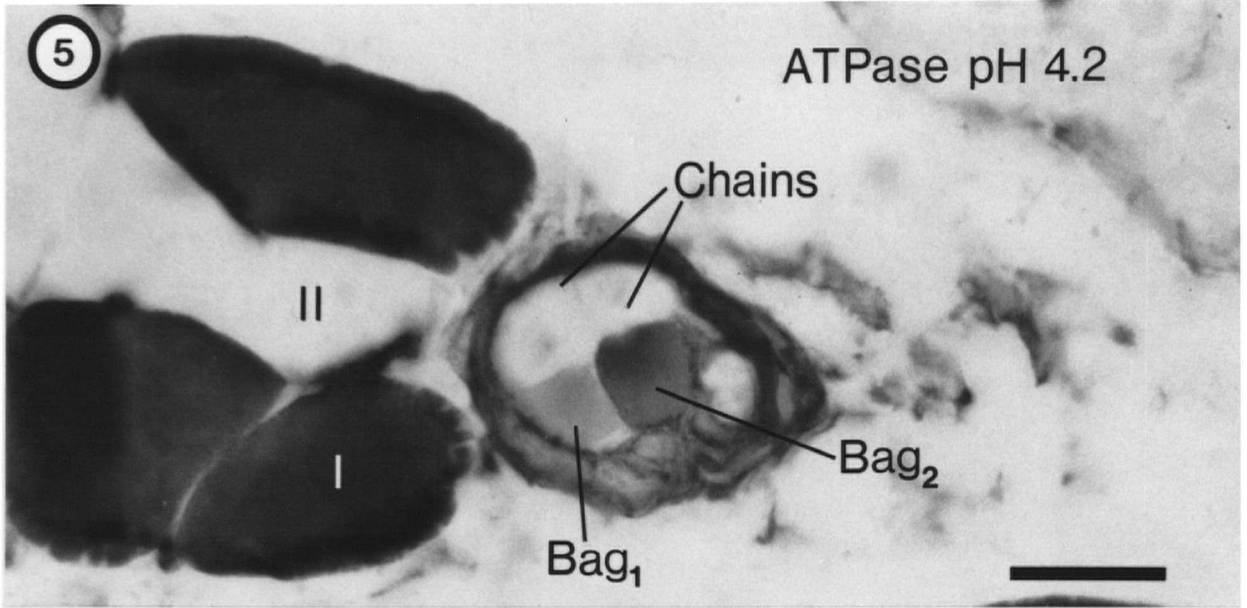
Number of spindles per muscle	range	16 - 20
	mean	18.4 ± 0.7
Intrafusal fibers per spindle	range	2 - 6
	mean	3.8 ± 0.09
Spindle length (mm)	range	4.7 - 12.2
	mean	7.5 ± 0.4
Tandem spindles per muscle	range	1 - 4
	mean	2 ± 0.7
Muscle spindle index (#/g muscle wt)		502.7

Figs. 5-7. Histochemical profiles of extrafusal and intrafusal muscle fibers in serial sections of the hamster tenuissimus. x1,050. Bars = 20 μ m.

Fig. 5. Myosin ATPase staining activity at pH 4.2. Type I extrafusal fibers stain darkly as does a bag₂ intrafusal fiber. Chain fibers along with type II extrafusal fibers are pale staining. A Bag₁ fiber exhibits intermediate staining properties.

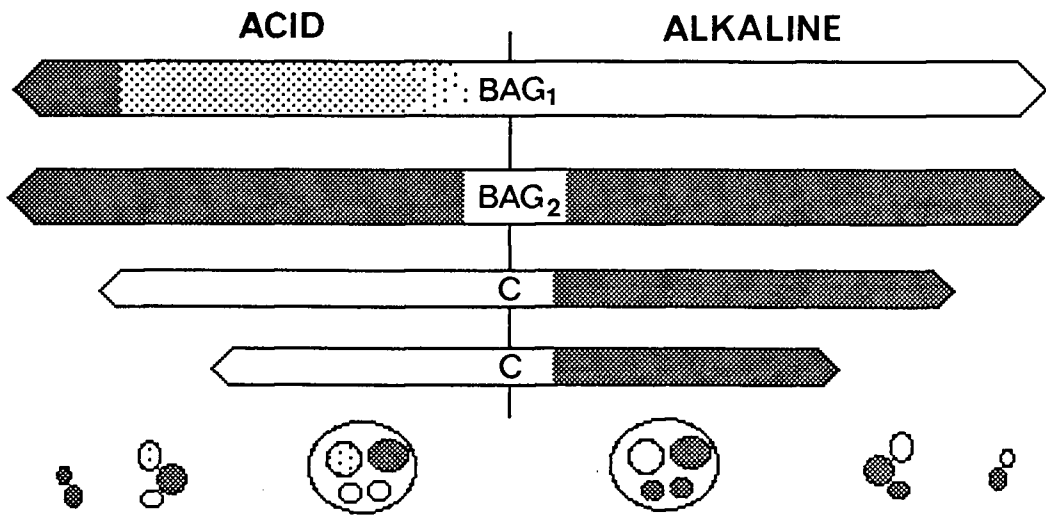
Fig. 6. Serial cross-section stained for myosin ATPase at pH 9.4. Extrafusal fibers and chain fibers show a complete reversal of staining properties. The Bag₁ fiber is alkaline-labile and is pale, whereas the bag₂ fiber is alkaline-stable and, again, stains darkly.

Fig. 7. Serial cross-section stained for NADH-TR activity. Both type I and type II extrafusal fibers stain moderately for this enzyme and differ very little from each other in their oxidative profiles. Large formazan granules can be seen within the sarcoplasm of the two chain fibers indicating high levels of oxidative activity. Both bag fibers stain less intensely although a few large formazan granules can be seen within the bag₂ fiber.



Figs. 8-9. Schematic illustrations of the overall myosin ATPase (Fig. 8) and NADH-TR (Fig. 9) staining properties of bag₁, bag₂, and chain fibers (C) in the tenuissimus muscle of the hamster. Figure 8 has been divided symmetrically at the equator to show the staining profiles of spindle poles under acid (left) and alkaline (right) preincubation conditions. Figure 9 shows the staining profiles along the length of each intrafusal fiber.

8



9

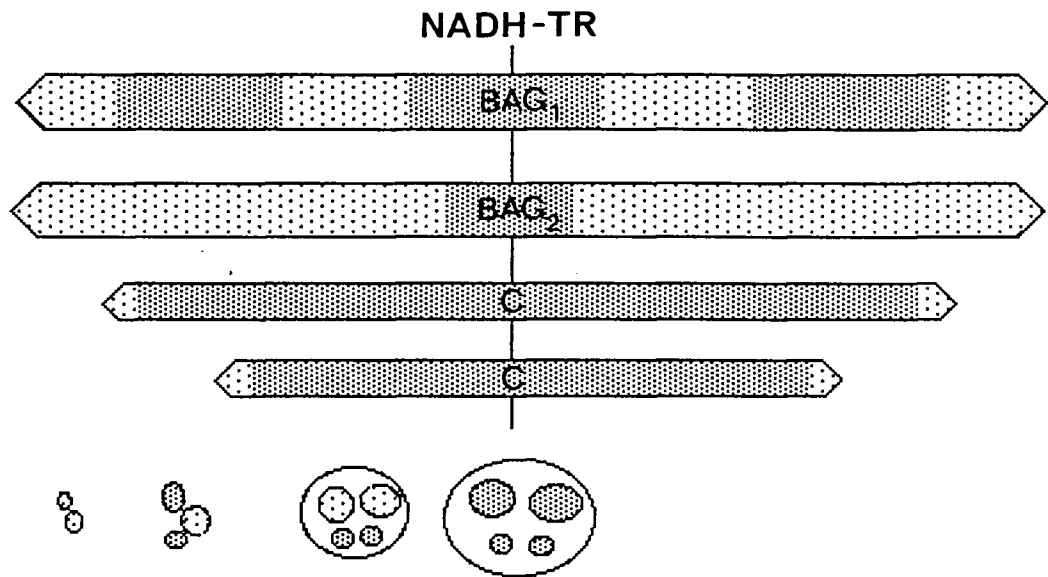


Fig. 10. Light micrograph of two isolated muscle spindles (numbered 1 and 2) arranged in tandem and viewed under darkfield illumination. An intrafusal fiber bundle (asterisk) can be seen coursing through the semitransparent and fusiform outer capsule (small arrows) of spindle #2. A small nerve bundle can be seen outside of the capsule in the juxtaequatorial region (curved arrow). The point of contact between the two spindles is indicated (circle). x350. Bar = 100 μ m.

Fig. 11. Fluorescence micrograph. Four intrafusal fibers are seen in this high magnification light microscopic view of an isolated muscle spindle treated with NBD-phalloidin. Two bag (asterisks) and two chain fibers (above) are present. The banding pattern of F-actin appears different for each of the four fibers. x2,240. Bar = 10 μ m.

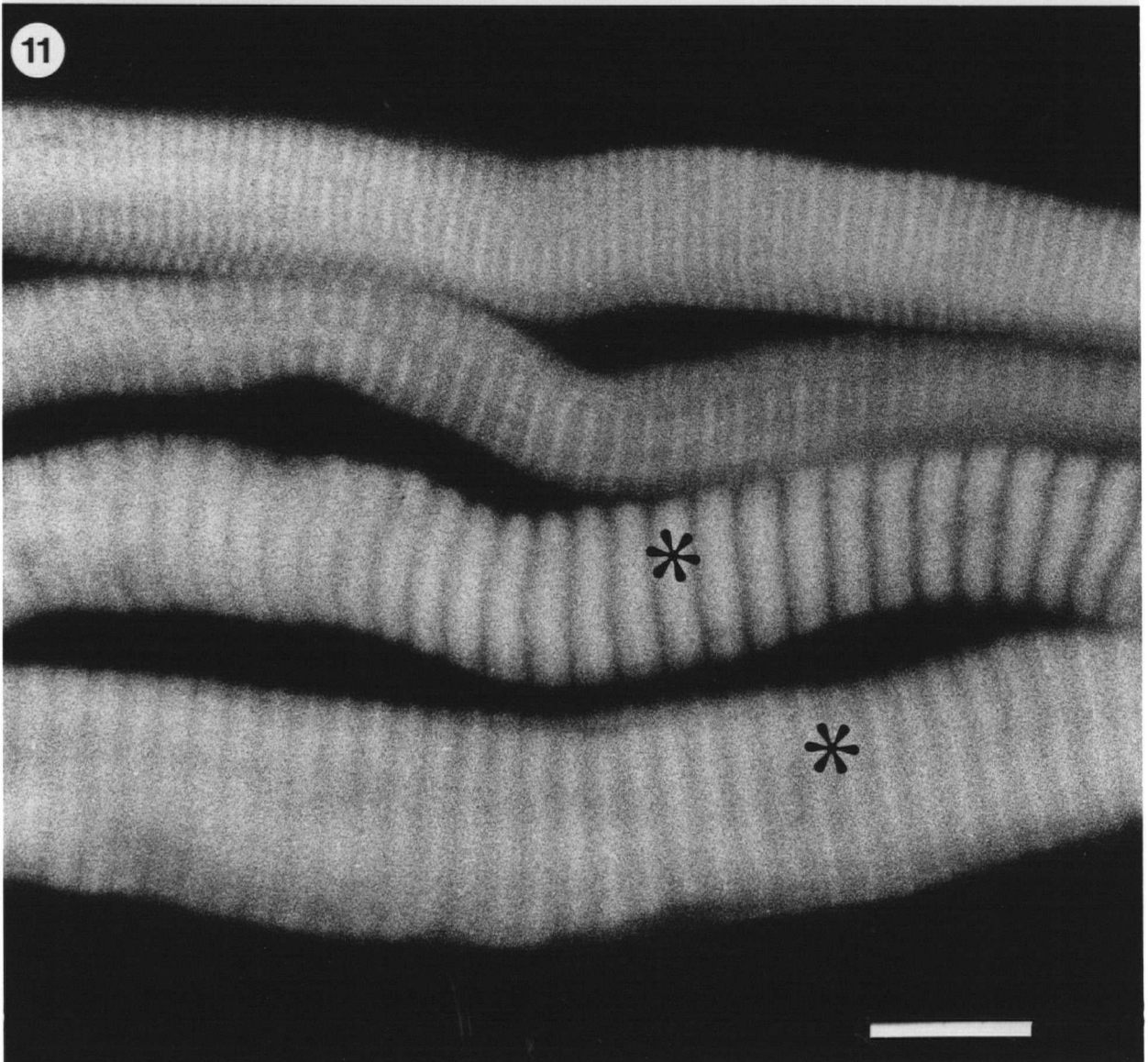
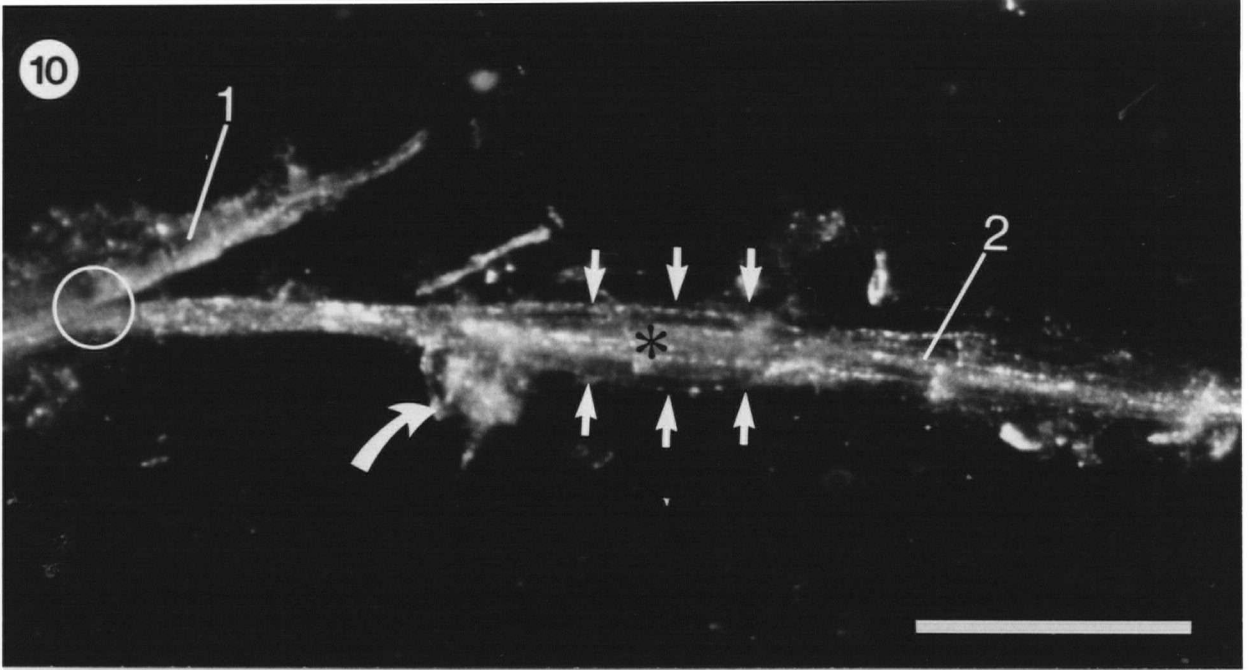


Fig. 12. High resolution scanning electron micrograph of a muscle spindle in the equatorial region. Three intrafusal muscle fibers are intimately enveloped by a delicate inner capsule. The external and internal surfaces of the multilayered outer capsule are covered by an intricate network of connective-tissue fibrils. Embedded within the capsular lamellae are profiles of three nerve fibers and a capillary (asterisk). x3,300. Bar = 10 μm .

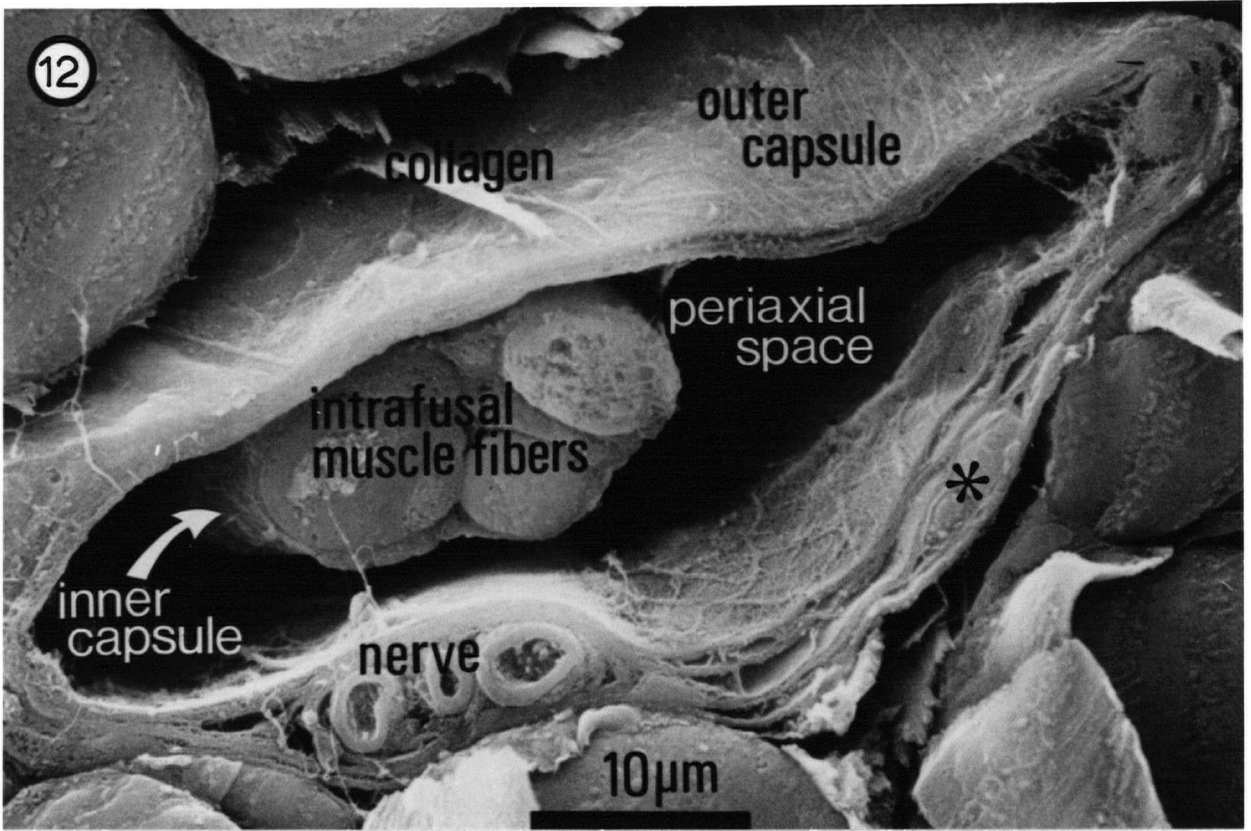
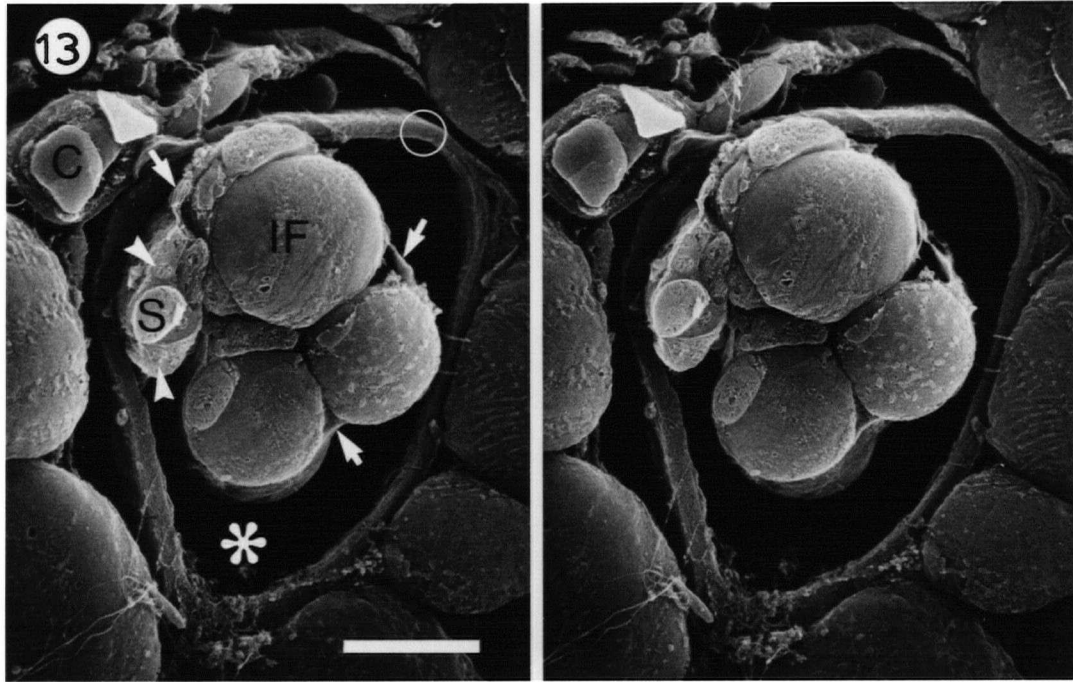


Fig. 13. High resolution SEM stereo pair of a muscle spindle in the juxtaequatorial region. Inner capsule cells and their processes (arrows) envelop three intrafusal fibers (IF). Several neuronal profiles (arrowheads) and an associated Schwann cell (S) are surrounded by the periaxial space (asterisk). A capillary (C) can be seen traversing the external surface of the outer capsule (circle). x1,800. Bar = 10 μ m.



Figs. 14-15. Conventional scanning electron micrographs of isolated spindles treated with 8N HCl. Both are viewed longitudinally in the juxtaequatorial region.

Fig. 14. A portion of the outer capsule of this spindle has been removed revealing a prominent sarcomeric banding pattern on the surfaces of two intrafusal fibers. Branching nerve fibers occupy what is left of the periaxial space. x9,600. Bar = 1.0 μm .

Fig. 15. The outer capsule appears directly continuous with the perineurial sheath of the nerve fascicle that supplies this spindle (double-headed arrow). The chemical treatment has partially digested away some capsule cells revealing their multilayered arrangement. A small capillary with an erythrocyte in its lumen (asterisk) has been cleaved open and is seen travelling in tandem with the perineurial sheath. x3,200. Bar = 5 μm .

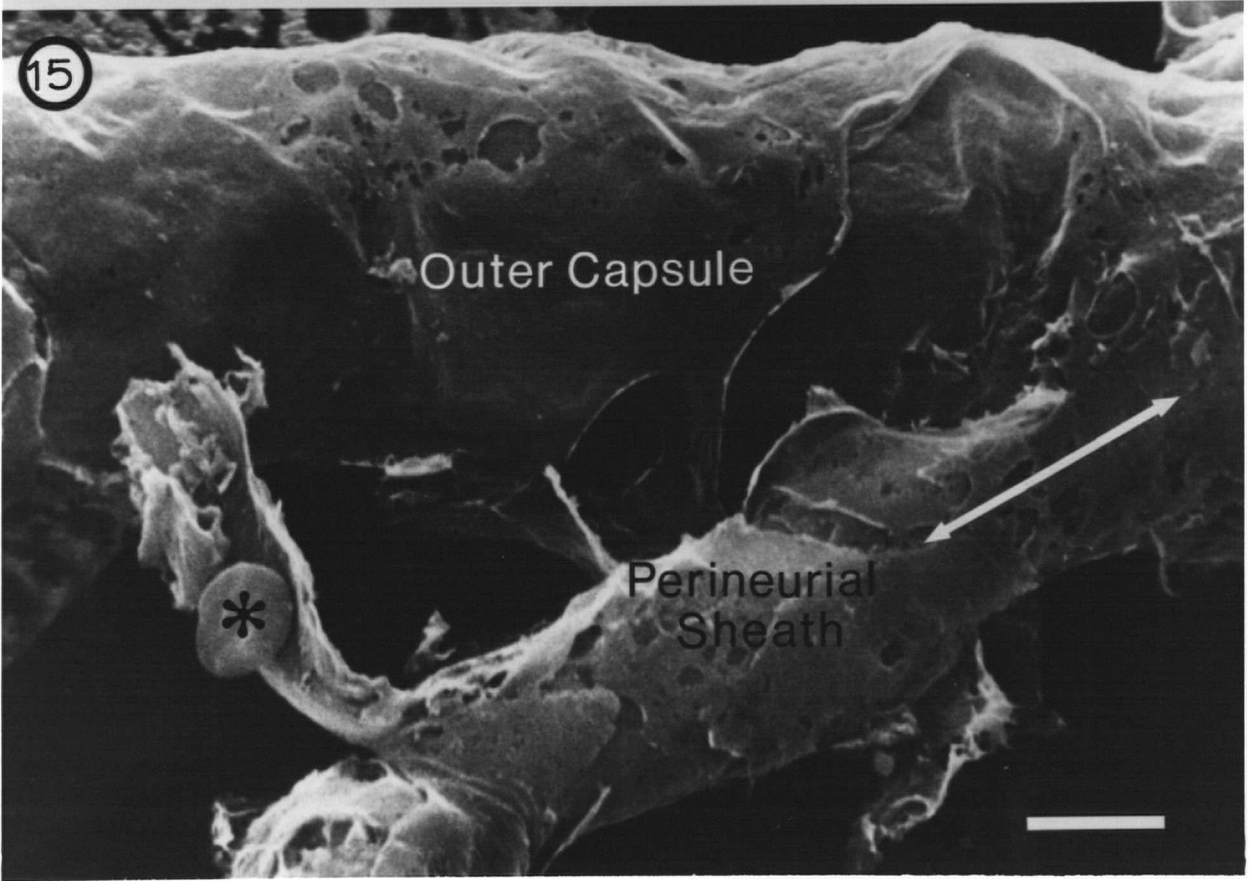
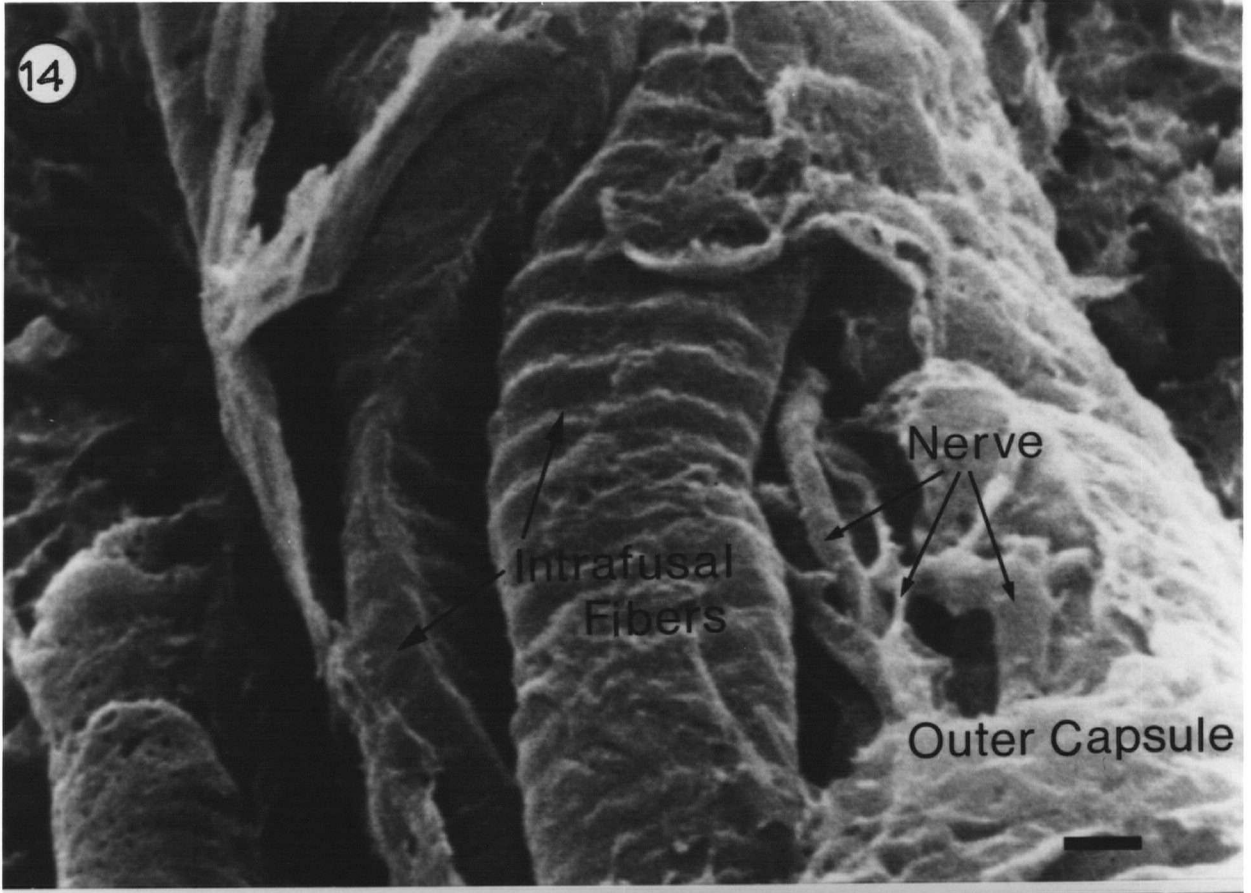


Fig. 16. The overall width of the outer capsule is seen in the transverse plane in this high resolution SEM. The capsule contains alternating layers of elongated and attenuated cells with intervening collagen fibrils (straight arrows). Within the cells, profiles of rough-surfaced endoplasmic reticulum (curved arrows), mitochondria, and a myriad of spherical transcytotic vesicles are evident. The external surface of the capsule (above) is covered by a dense meshwork of collagen fibrils. x22,100. Bar = 1.0 μm .

Fig. 17. High resolution SEM showing three layers of the outer capsule cleaved longitudinally (numbered 1-3). Cellular morphology varies according to individual layers. Long cytoplasmic processes resembling filopodia (arrows) intermingle with a network of collagen fibrils. An abundance of small microvillus-like surface-projections stud the external surfaces of some cells. x13,400. Bar = 1.0 μm .

Fig. 18. Higher magnification view of the region outlined in the rectangle in Figure 6. Collagen fibrils show an interwoven pattern amongst the cytoplasmic processes of adjacent capsular cells. Many small surface-projections of these cells (straight arrows) and transcytotic vesicles (curved arrows) are also seen. x40,400. Bar = 0.5 μm .

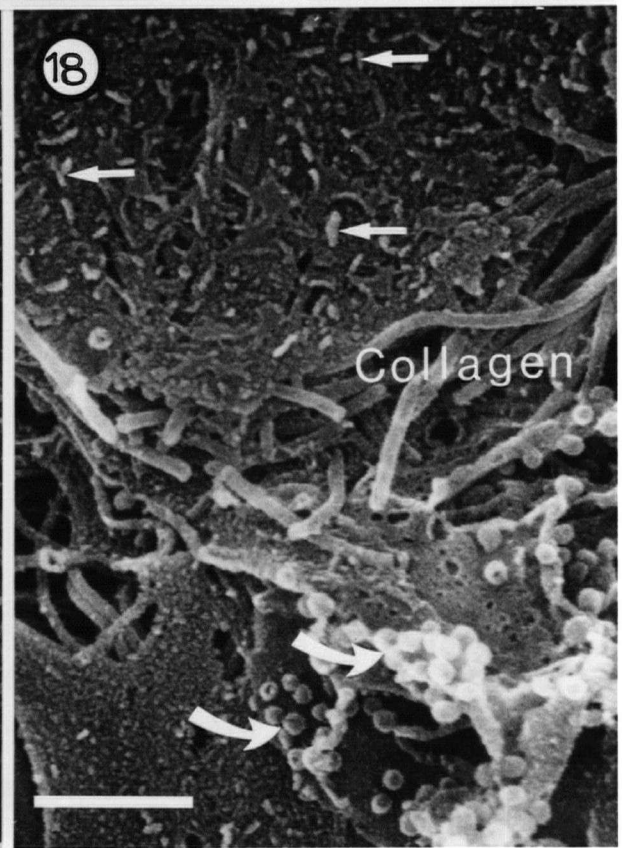
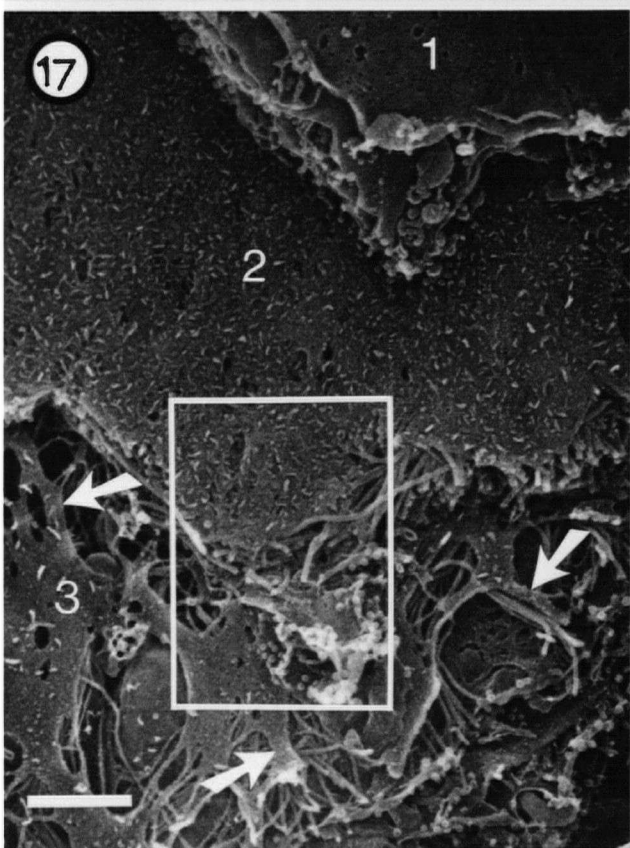
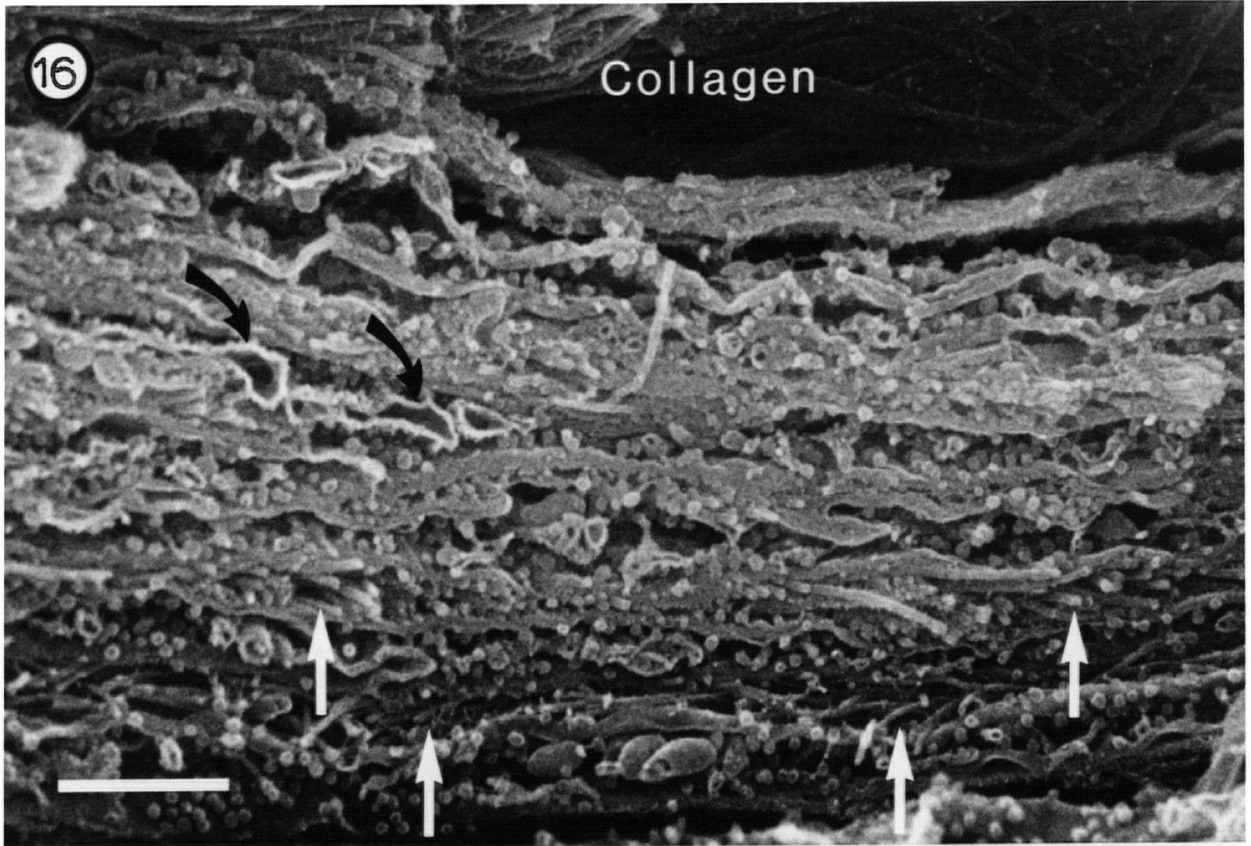


Fig. 19. The inner capsular sheath of a single intrafusal fiber is revealed longitudinally in this HRSEM. It is partially peeled away and shows that the outer surface of the muscle fiber is covered by a prominent external lamina composed of an interwoven meshwork of connective-tissue fibrils. Within the inner capsule, a single row of elongated mitochondria are stacked in parallel with the longitudinal axis of the spindle (circle). x13,600. Bar = 1.0 μm .

Fig. 20. A cross-sectional view of part of an inner capsule cell is illustrated in this HRSEM. Rough-surfaced endoplasmic reticulum (curved arrow) and an elaborate Golgi complex with associated vesicles and vacuoles are in the perinuclear cytoplasm. x42,000. Bar = 0.5 μm .

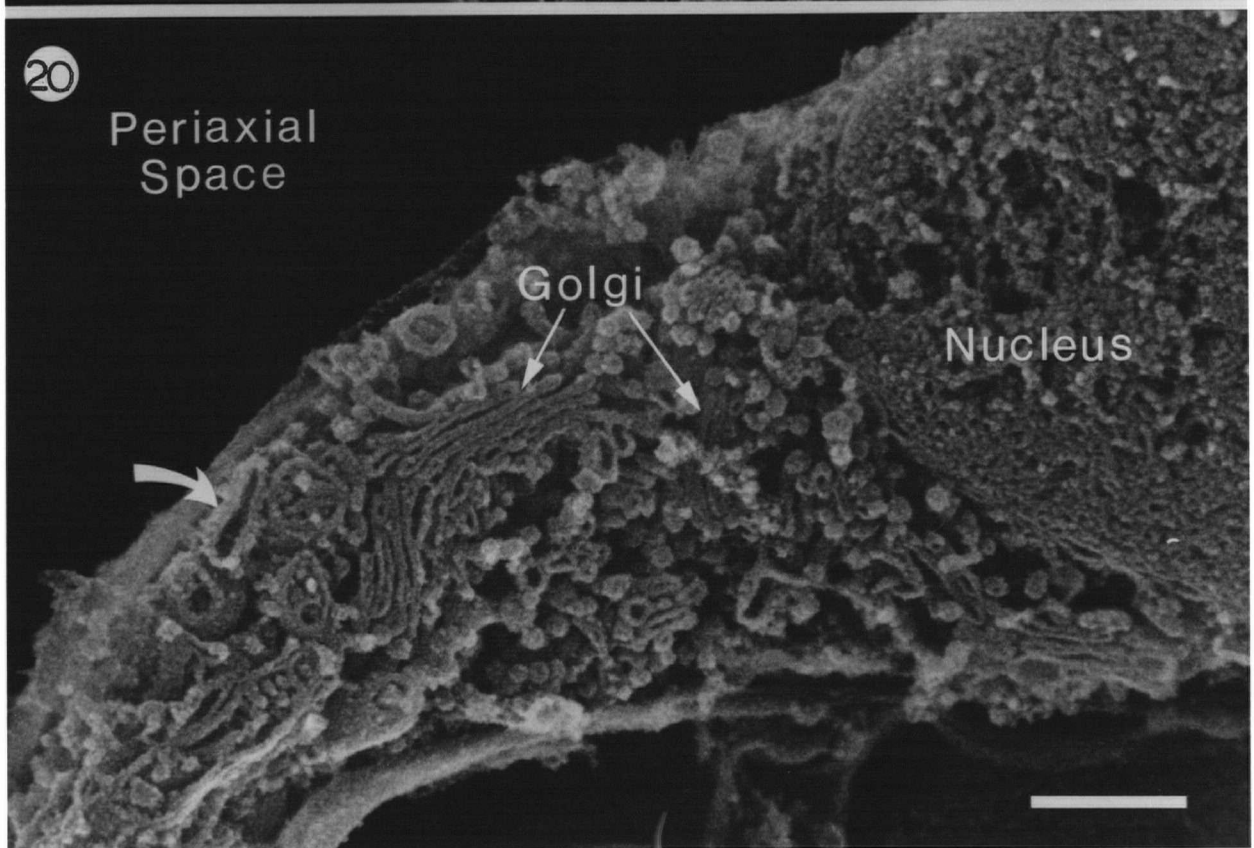
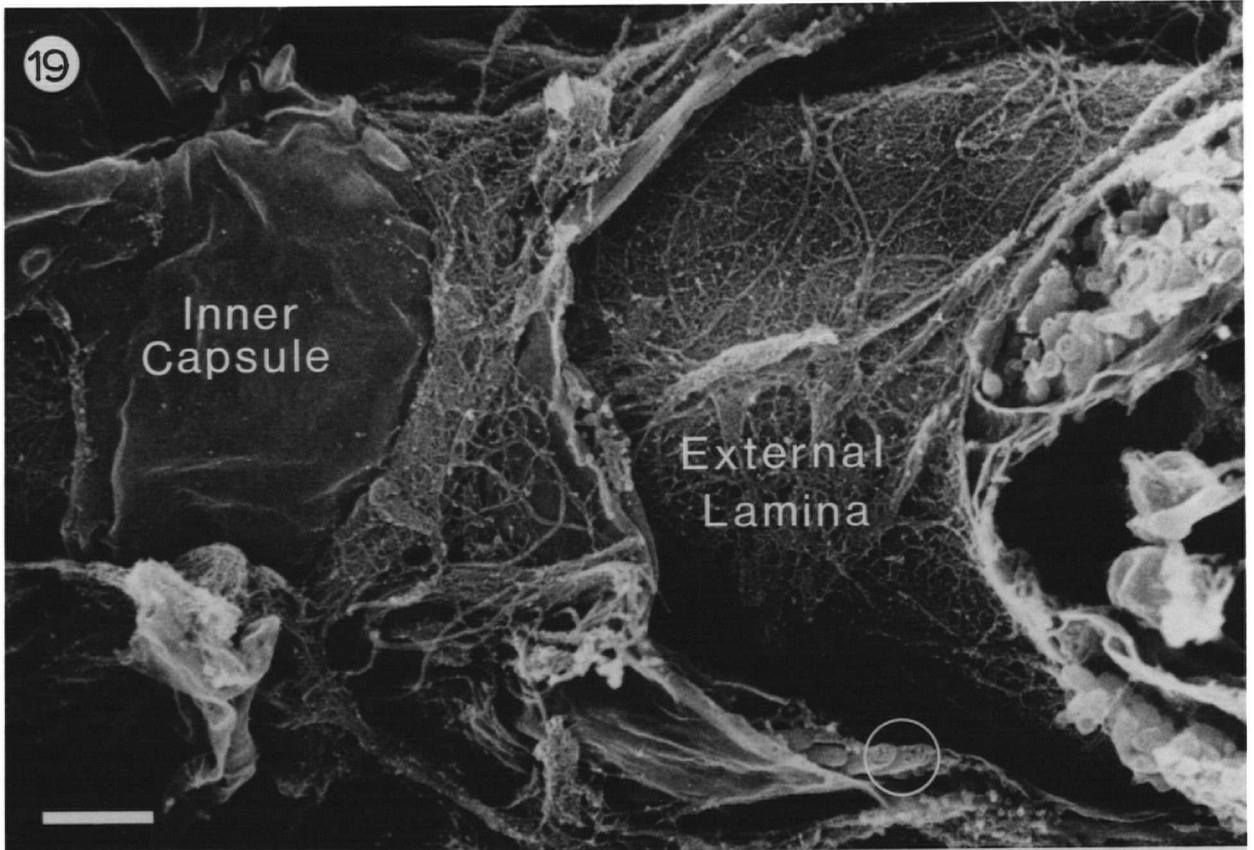


Fig. 21. A fusimotor nerve ending sitting on the surface of an intrafusal fiber is depicted in this high resolution SEM. The nerve terminal has been cleaved open revealing mitochondria (star) and synaptic vesicles (straight arrows) in the axoplasm. Within the muscle fiber, small mitochondria (arrowheads) and dilated cisternae of the SR (asterisks) occupy the region just below the sarcolemma. The process of a Schwann cell is also seen on the outer surface of the nerve ending. x35,000. Bar = 1.0 μm .

Fig. 22. High resolution SEM showing details of a sensory nerve ending viewed in cross-section. The crescent-shaped terminal contains numerous mitochondria and cytoplasmic vesicles, and lies in close apposition to an intrafusal fiber. Note the tightly-packed myofilament lattice in the sarcoplasm of the intrafusal fiber. x28,800. Bar = 1.0 μm .

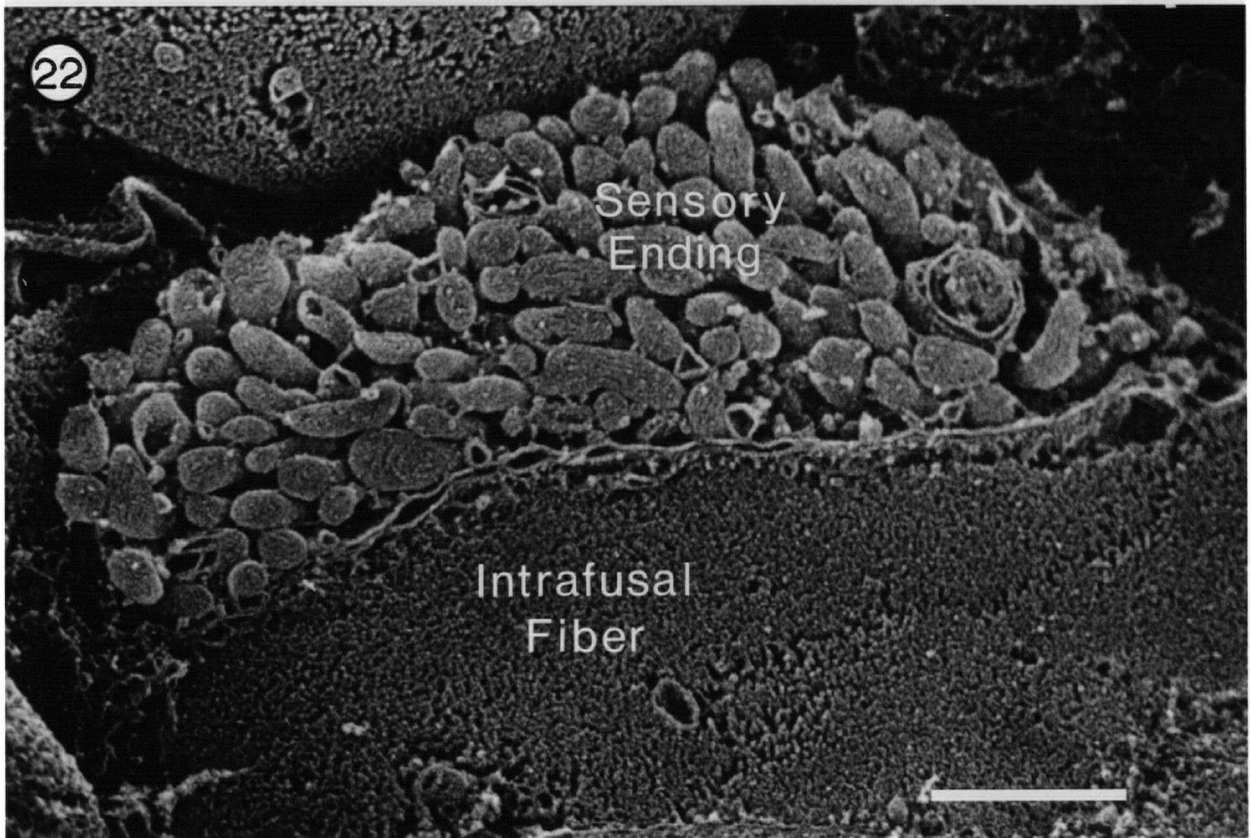
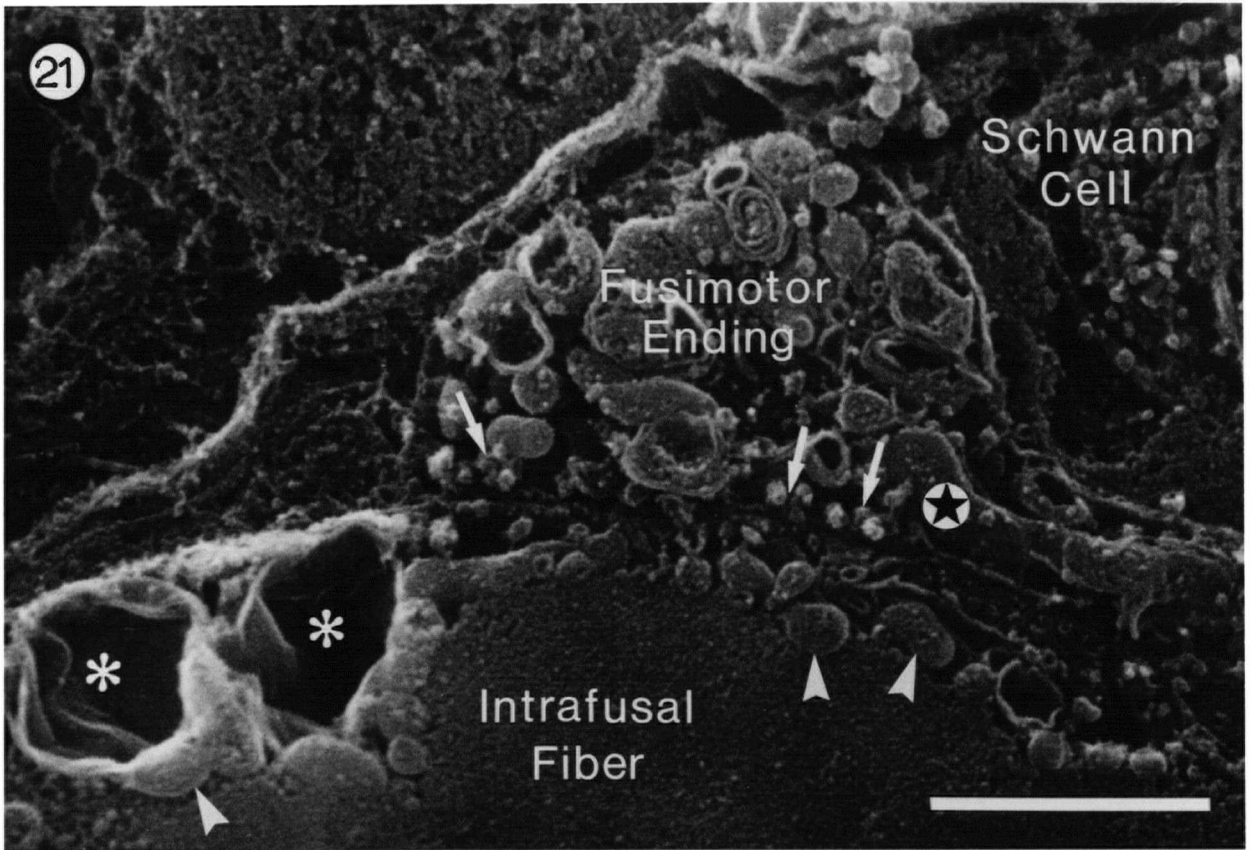
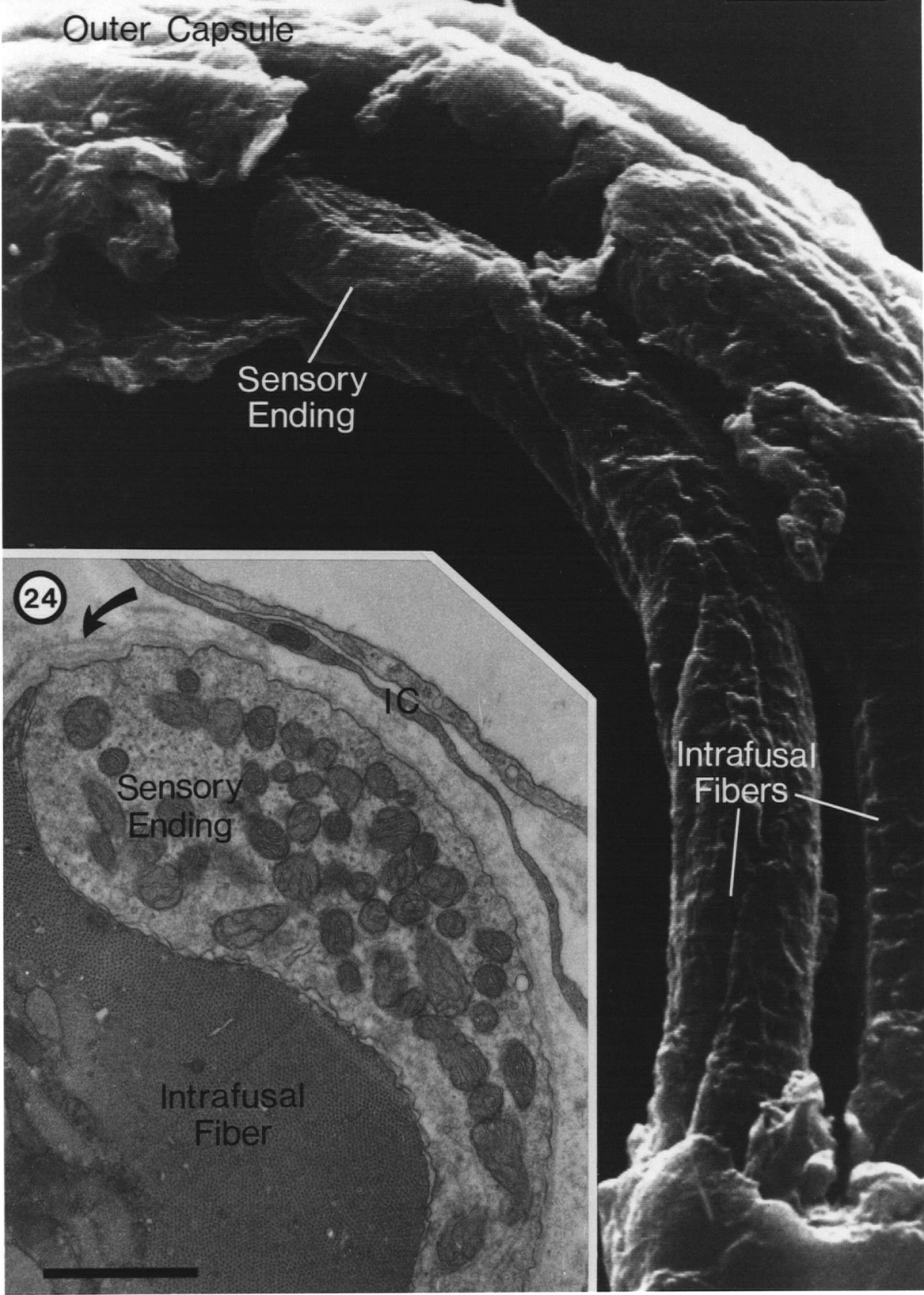


Fig. 23. Conventional SEM of an isolated muscle spindle whose outer capsule has been partially removed. A sensory nerve ending appears as a punctate expansion sitting on the surface of an underlying intrafusal fiber. x5,700. Bar = 5 μm .

Fig. 24. TEM view of a sensory nerve ending on an intrafusal fiber cut in cross-section. The sensory ending is crescent-shaped and sits in a shallow depression on the surface of the intrafusal fiber. The outer neuronal membrane appears corrugated and is covered by external lamina (curved arrow). Microtubules, neurofilaments and many rounded mitochondrial profiles are present within the axoplasm. Cytoplasmic extensions of two inner capsule cells (IC) are also indicated. x27,250. Bar = 1.0 μm .

23



24



Fig. 25. High magnification SEM stereo pair detailing the intimate relationship between a sensory ending (SE) and an underlying intrafusal fiber (IF). Specialized areas of contact (arrows) appear to link the nerve cell membrane and the underlying sarcolemma. Three membrane-bounded tubular profiles (arrowheads) lie closely apposed to the nerve cell membrane. x31,800. Bar = 0.5 μm .

Fig. 26. High resolution SEM. The elongated and tightly-packed nature of the mitochondria are illustrated in this stereo pair image of a sensory nerve ending (SE). Many cytoplasmic filaments are attached to the neuronal cell membrane (arrows). A delicate extracellular meshwork characterizes the overlying external lamina (EL). x11,800. Bar = 1.0 μm .

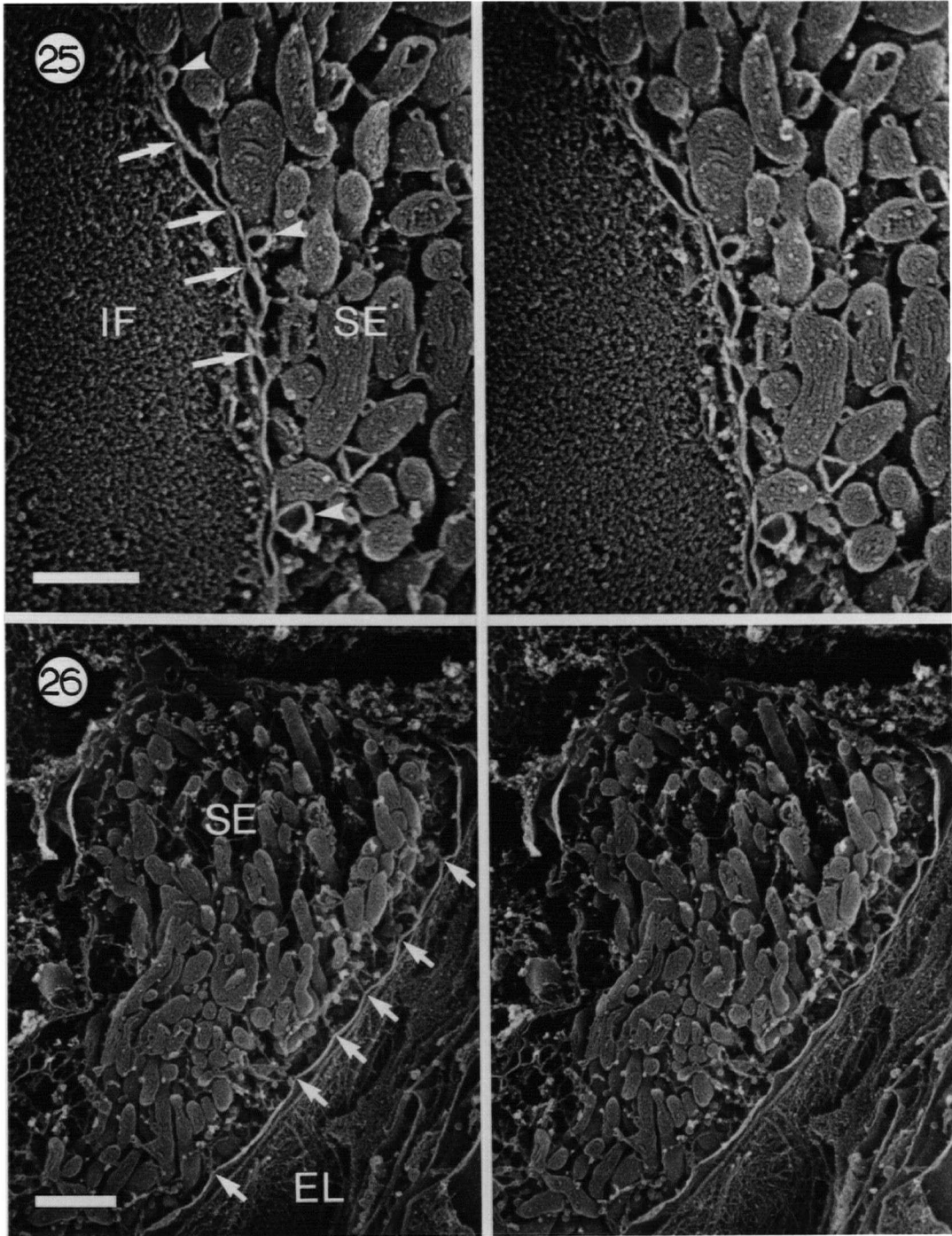


Fig. 27. High resolution SEM of the interior of a crescent-shaped sensory ending that has been fractured open. Vesicles (arrowheads) occupy the axoplasm, and mitochondria are cleaved open at different levels revealing their inner cristae (curved arrows). Sites of intimate contact between the nerve cell membrane and the sarcolemma are evident (circles). The myofilaments in the sarcoplasm of the underlying intrafusal fiber have been selectively extracted (asterisk). Elements of the SR in the muscle cell are seen in close association with the sarcolemma (arrows). A subsarcolemmal T-tubule is also indicated (T). x67,500. Bar = 0.5 μm .

